



Research Article

Compositional Chemical Property Analysis and Evaluation of Liquid Smoke Produced from Microwave-assisted Pyrolysis of Mixtures of Oil Palm Solid Waste

Wahyu Meka, Orchidea Rachmaniah*, Berlian Widi Bela Pamungkas, Faisal Akbar, Adidoyo Prakoso, Latifa Hanum Lalasari, Sri Fitria Retnawaty, Shanti Faridah binti Salleh, Salman Masoudi Soltani, and Paul Fennell

Received: May 23, 2025 | Revised: July 20, 2025 | Accepted: July 30, 2025 | Online: August 21, 2025

Abstrac

Microwave-assisted pyrolysis (MAP) was employed to valorise oil palm solid waste, namely empty fruit bunches (EFBs), kernel shells (KSs), and mesocarp fibres (MFs), into liquid smoke at 300 and 400 °C. Unlike conventional pyrolysis systems, which rely on slow, external heating and often yield broad, less selective chemical profiles; MAP offers rapid, volumetric heating and nonthermal effects that enhance product specificity and energy efficiency. This study investigates how MAP temperature and binary blending ratios (EFB-to-KS and EFB-to-MF) influence liquid smoke yield, chemical composition, and antioxidant capacity. Liquid smoke yields were significantly affected by temperature in EFB-KS mixtures, with higher yields at 400 °C, while EFB-MF mixtures showed yield stability across conditions. Gas chromatography-mass spectrometry (GC-MS) analysis revealed phenol as the dominant compound across all samples, with compound diversity and antioxidant activity varying by feedstock. KS-rich mixtures favoured catechol and cresol formation, MF-rich mixtures produced cyclopentenones and carboxylic acids, and EFB-rich mixtures yielded more carbonyl-containing compounds. Antioxidant capacities, measured via DPPH assay, were highest in KSderived liquid smoke due to its catechol content, while EFB-rich samples exhibited lower activity. Principal component analysis (PCA) was applied to GC-MS data to elucidate the chemical transformation pathways, revealing distinct degradation routes for cellulose, hemicellulose, and lignin under MAP conditions. These routes were further supported by compound clustering in PCA loading plots, highlighting the influence of temperature and biomass composition on product speciation. This study demonstrates the innovative integration of MAP with oil palm waste valorisation, offering a sustainable alternative to wood-based pyrolysis. By tailoring feedstock ratios and operating temperatures, MAP enables the targeted production of high-quality liquid smoke with enhanced antioxidant functionality, contributing to environmentally friendly food preservation and agricultural applications.

Keywords: pyrolysis, microwave, oil palm, liquid smoke, agricultural waste

1. INTRODUCTION

A growing interest in healthy diets has led to increase consumer preference for organic food. Global organic food retail sales rebounded to about EUR 136.4 billion in 2023, marking renewed growth after a 2022 slowdown [1]. Although demand for organic animal-based foods remains lower than that for plant-based alternatives, they are expected to become staple items in future diets [2]. However, due to their limited shelf life, most organic foods require natural preservatives to maintain their organic status [3]. One of the most widely recognised natural preservatives in global

Publisher's Note:

Pandawa Institute stays neutral with regard to jurisdictional claims in published maps and institutional affiliations.



Copyright:

© 2025 by the author(s).

Licensee Pandawa Institute, Metro, Indonesia. This article is an open access article distributed under the terms and conditions of the Creative Commons Attribution (CC BY) license (https://creativecommons.org/licenses/by/4.0/).

food markets is liquid smoke, traditionally produced from wood through pyrolysis followed by condensation. When applied to food, liquid smoke not only preserves it but also enhances flavour and colour [4]. Beyond food applications, it has also been used in agriculture for crop fertilisation and pest control [5]. According to Grand View Research, the widespread use of liquid smoke across various industries has expanded its global market to over USD 50 million in the past decade [6].

Wood pyrolysis has become the predominant method for producing liquid smoke, replacing earlier techniques such as smouldering—slow wood combustion under limited oxygen—followed by smoke condensation [7]. This transition was driven by improved efficiency and reduced emissions of greenhouse gases and pollutants such as CO and NOx. Pyrolysis involves the thermal, anaerobic decomposition of wood into gaseous, liquid, and solid products at temperatures ranging from 300 to 500 °C [8]. Compared to smouldering, pyrolysis offers superior yield, better control over product quality, and reduced environmental impact [9]. Despite its effectiveness, continued reliance on

Table 1. General lignocellulosic material pyrolysis settings for high selectivity liquid smoke.

Parameter	Level
Pyrolysis temperature	High*
Cellulose Content of the Lignocellulosic Material	High
Hemicellulose Content of the Lignocellulosic Material	High
Lignin Content of the Lignocellulosic Material	Low
Guacyl Unit Content of the Lignocellulosic Material	Low
Syringil Unit Content of the Lignocellulosic Material	High
p-Hydroxyphenyl Unit Content of the Lignocellulosic Material	High

^{*} not more than 600 °C promoting formation of CO and CO2 due to rapid and extreme heating.

wood as a feedstock poses environmental risks, including deforestation and its contribution to global warming [10]. Diminished tree populations also compromise forest ecosystems by reducing erosion control, biodiversity, and watershed quality [11]. Therefore, identifying sustainable alternatives to wood is essential.

Oil palm (*Elaeis guineensis*) solid waste presents a promising substitute. These lignocellulosic materials exhibit similar thermal behaviour during pyrolysis and are abundantly available. Global oil palm production has increased by over 70 million tonnes since 1961 [12], with Indonesia leading as the largest producer. In recent years, Indonesia has generated over 260 million tonnes of oil palm solid waste annually, comprising 14.6% empty fruit bunches (EFBs), 8.3% mesocarp fibres (MFs), 4% kernel shells (KSs), 49.9% fronds and leaves combined, and 23.1% trunks [13]. While concerns about oil palm sustainability persist, this study focuses solely on the valorisation of waste materials that would otherwise be discarded. Pyrolysis has long been used to thermally convert oil palm solid waste, though most studies have targeted biofuel production. Only a few have explored optimising liquid smoke yield and composition. Although both biofuel and liquid smoke are produced via pyrolysis, they differ significantly in chemical characteristics and require distinct operating conditions, and reactor designs to enhance product selectivity. Liquid smoke production has been attempted using various reactor types. Kilns, which operate at slow heating rates, are cost-effective and suitable for large biomass volumes but offer limited control over product selectivity [14]. Fluidised-bed reactors, with faster heating rates, are preferred when liquid products are the primary target [15], though they are complex to operate, difficult to scale up, and expensive to maintain [16].

have Recent advancements introduced microwave-assisted pyrolysis (MAP) reactors, which offer several advantages over conventional systems. These include extremely rapid heating, efficient energy use, and simplified operational control [17]. MAP is particularly suitable for food processing, as it avoids direct contact between the heating source and the biomass [18]. However, current MAP systems are limited to small-scale applications, necessitating further research and development for industrial-scale deployment. The contrasting heating principles of MAP and conventional pyrolysis give rise to significant differences in system behaviour, including feedstock suitability, operational parameters, and potentially the reaction mechanisms involved. Conventional pyrolysis generally requires pre-dried biomass, whereas MAP can effectively process raw biomass with higher moisture content. This is because water, a polar molecule, strongly interacts with microwave radiation, enabling internal heat generation. Heat absorption in MAP can also be enhanced using microwave-absorbing materials such as biochar, which function as absorbers to facilitate rapid and uniform heating [19][20].

Temperature regimes further distinguish the two approaches. Conventional pyrolysis typically operates at elevated temperatures between 300 and 900 °C, while MAP is often categorised as a low-temperature pyrolysis process, generally conducted within the 180–500 °C range [21]-[23]. In terms of heat transfer, conventional systems rely on conductive heat from external sources, progressing



inward. In contrast, MAP initiates heating from within the biomass due to microwave interaction with polar components, with thermal propagation moving outward [24]. MAP offers not only thermal effects but also non-thermal effects, such as the microwave-induced rotation and excitation of polar functional groups, which may influence reaction kinetics and product distributions [25]. These nonthermal effects are reflected in the different chemical profiles of the liquid smoke. For instance, pyrolysis of amorphous cellulose conventional heating tends to favour the formation of phenolic compounds, while microwave pyrolysis results in higher yields of furanic products [26]. Moreover, in the presence of moisture, MAP promotes hydrolytic degradation reactions that enhance the production of sugars, furans, and levulinic acid [27]. In the case of lignin, microwave treatment produced liquid smoke enriched with phenol, hydrocarbons, and esters, in contrast to the guaiacol-dominant products typically observed in conventional pyrolysis [28].

This study explores the potential of MAP for producing liquid smoke from oil palm solid waste. Binary mixtures of oil palm waste materials were selected as feedstocks, as previous research has predominantly focused on the pyrolysis of individual waste types, such as EFBs, KSs, and MFs [29]-[33]. In this study, both the composition of the waste mixtures and the pyrolysis temperatures were systematically varied to assess their effects on liquid smoke yield, chemical composition, and antioxidant capacity. To establish a comparative framework, Tables 1 and 2 present

the typical characteristics of liquid smoke derived from conventional pyrolysis of lignocellulosic biomass. These serve as a baseline for evaluating the performance and selectivity of MAP under the conditions investigated [34].

2. MATERIALS AND METHODS

2.1. Raw Material Preparation

Raw materials were solid wastes of oil palm trees from Kalimantan provided by Agro Indomas (an Indonesian private plantation company). The raw materials comprised several oil palm solid waste types: EFBs, KSs, and MFs. The oil palm solid waste types were milled to below a 60-mesh particle size to improve heat and mass transfer rates within raw materials during pyrolysis. Ground active carbon with a particle size of 2 mm was mixed with the oil palm solid waste types in each pyrolysis run to provide microwave absorbance.

2.2. Raw Material Characterisation

Each oil palm solid waste type was characterised via proximate analysis, ultimate analysis, and thermogravimetric analysis. Proximate analysis (on a % a.r. basis) was conducted to measure moisture, volatile matter, fixed carbon, and ash content. Ultimate analysis (on a % d.a.f. basis) was conducted to measure carbon, hydrogen, nitrogen, sulphur content. Moisture and content determination was conducted following procedure outlined in ASTM D 3173. 1 g of milled sample of EFBs, KSs, or MFs, was weighed into pre-dried, pre-weighed capsules. The capsules had

Table 2. General selectivity of chemical compound group in liquid smoke produced from lignocellulosic material component pyrolysis.

Component		Temperature ra	ange (°C)	
Component	200–300	300–400	400–500	>500
Cellulose	No formation, depolymerisation occurs	Monomeric sugars, such as levoglucosan	Furanic compounds and carbonyl- containing compounds	Strong vaporisation
Hemicellulose	No formation, depolymerisation occurs	Anhydrosugars	Furanic compounds and carbonyl- containing compounds	Strong vaporization
Lignin	No formation, cleavage of carbon-carbon bond and carbon-oxygen bond	Methoxyphenols	Phenols, alkylphenols, and aliphatics	Strong vaporisation

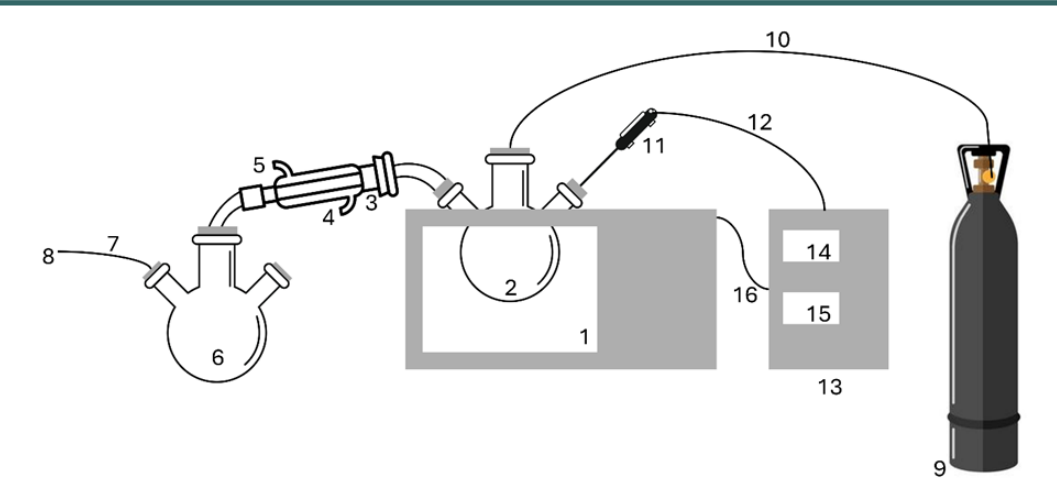


Figure 1. Experimental setup of microwave-assisted pyrolysis (MAP): (1) microwave oven, (2) three-neck round-bottom flask, (3) Liebig condenser, (4) Liebig condenser annulus outlet, (5) Liebig condenser annulus inlet, (6) three-neck round-bottom flask to collect liquid products, (7) plastic hose, (8) outlet flow of non-condensable gas, (9) cylinder of nitrogen, (10) plastic hose, (11) thermocouple probe, (12) electrical cable, (13) control box, (14) temperature display, (15) wattage display, and (16) electrical cable.

been heated under the same conditions as used for drying the sample, cooled in a desiccator for 15 to 30 min, and weighed before use. After sample loading, the capsules were immediately reweighed to minimise moisture loss due to ambient exposure. The sample were then dried in a preheated oven at 110 °C for 1 h in the presence of a flow of dry air. Upon completion, the capsules were removed from the oven, promptly covered, cooled in a desiccator, and reweighed at room temperature. The moisture content was calculated based on the weight difference before and after drying.

Volatile matter content determination was performed in accordance with ASTM D 3175. 1 g of milled sample of EFBs, KSs, or MFs was weighed into a pre-weighed platinum crucible fitted with a closely matching lid to prevent air ingression. The crucible was placed on platinum wire supports and introduced directly into a muffle furnace maintained at 950±20 °C. The sample was quickly lowered to the high-temperature zone to initiate pyrolysis. After 7 min of heating, the crucible was removed from the furnace and allowed to cool to room temperature without disturbing the lid. Cooling was performed in a desiccator to prevent moisture uptake. The crucible was then reweighed, and the percentage of volatile matter was calculated based on the weight loss, excluding the previously determined moisture content.

Ash content determination was carried out

following the procedure outlined in ASTM D 3174. 1 g of milled sample of EFBs, KSs, or MFs transferred into a pre-weighed ceramic boat. The ceramic boat was initially placed in a cold muffle furnace, which was then heated gradually to reach a temperature of 450–500 °C within 1 h. The temperature was then increased to a final set point of 750 °C and maintained for an additional 2 h, allowing for complete combustion of the organic matter. After the heating period, the ceramic boat was removed, covered immediately to minimise moisture uptake, cooled to room temperature in a desiccator, and reweighed. The ash content was calculated based on the residue remaining after combustion.

Carbon, hydrogen, and nitrogen contents were measured with Sundy SDCHN435u which met ASTM D 5373 and GB/T 30733-2014. 100 mg of milled sample of EFBs, KSs, or MFs was introduced to the equipment. The measurement was conducted according to the manual instruction of the equipment for 8 min for each sample. Sulphur content was determined based on the procedure outlined in ASTM D 4239. 0.5 g of milled sample of EFB, KS, or MF evenly spread into a combustion boat, optionally lined with a thin layer of Al₂O₃ to prevent sample loss during combustion. The sample was introduced into a horizontal tube furnace preheated to 1350 °C, with a continuous flow of oxygen at approximately 2 L/min. The combustion



sequence involved a staged heating approach: the sample boat was first held at the inlet for 3 minutes to release volatiles, then gradually moved toward the furnace's hot zone over 6 min and finally held in the centre for an additional 3 min to ensure complete oxidation of sulphur to SO₂ and SO₃. Combustion gases were carried through a H₂O₂ absorption solution, where they were converted to H₂SO₄. The resulting acid was titrated using 0.05 M NaOH to determine the sulphur content.

Thermogravimetric analysis (TGA) was performed using a Mettler Toledo TGA/DSC 1. A 1 -g sample of each type of oil palm solid waste was placed in an Al₂O₃ crucible and heated from 30 to 1000 °C at a steady rate of 10 °C/min, under a consistent nitrogen flow of 20 mL/min.

2.3. Experimental Setup and Procedure

The laboratory-scale MAP system, depicted in Figure 1, comprised a modified microwave oven (labeled as number 1) and a control box (number The microwave oven, an Electrolux EMM20K22BA model, had five available distinct power settings: Melt (136 W), Defrost (264 W), Simmer (440 W), Reheat (616 W), and Quick Cook (800 W). A hole was made at the top of the microwave oven to accommodate a three-neck round-bottom flask (number 2). The left, center, and right necks of the flask were connected to a Liebig condenser inlet (number 3), a nitrogen cylinder (number 9) via a plastic hose (number 10), and a thermocouple probe (number 11), respectively. The ceramic-coated thermocouple probe measured the temperature and transmitted the data (number 12) to the control box (number 13), which then sent a correction signal (number 16) back to the microwave oven to adjust microwave output from the magnetron as needed. During condensation, cooling water continuously flowed through the

Liebig condenser from its annulus inlet (number 5) to its annulus outlet (number 4). The outlet of the Liebig condenser (number 2) was attached to the central neck of another three-neck round-bottom flask (number 6). In this flask, the right neck was sealed, while the left neck was used to expel gas through a plastic hose (number 7) that led out of the system (number 8).

The microwave was operated at constant temperatures 300 and 400 °C. These temperatures correspond to the primary thermal degradation ranges of hemicellulose (210-310 °C), cellulose (300-380 °C), and lignin (300-500 °C), which are the major components of EFBs. At approximately 300 °C, the decomposition of hemicellulose and cellulose is favoured, leading to the release of volatile compounds including acetic acid, furfural, and light ketones. At 400 °C, further thermal degradation of lignin occurs, promoting the formation of valuable aromatic phenolics such as guaiacol, syringol, and their derivatives, which contribute to the antioxidant, antimicrobial, and organoleptic properties of the resulting liquid smoke. Before pyrolysis, the set-point temperature at the control panel and the power level were set at 100 °C and Melt (150 W), consecutively, to gradually raise the oil palm waste type temperature until 100 °C. Along with this setup, the timer was set by 5 min to accommodate the entire microwave activity. Once 100 °C was achieved, the set-point temperatures and the power level were increased to the operating temperatures and Simmer (440 W). The change to this new set condition allowed the oil palm waste type temperatures to rise to the operating temperatures in less than 1 min. This new condition was hold for roughly 3 min which was sufficient to completely pyrolyse the entire oil palm solid waste types. After the pyrolysis, the microwave door was opened to turn off the

Table 3. Proximate and ultimate analysis results of oil palm solid waste.

Solid Waste	Pr	oximate An	alysis (% a	.r.)		Ultimate	Analysis	(% d.a.f.)	
Sonu waste	M	VM	FC	A	C	N	Н	S	O
EFB	16.15	61.36	17.27	5.22	52.46	0.73	6.03	0.28	40.50
KS	18.84	61.02	17.48	2.66	55.54	0.37	5.8	0.04	38.25
MF	17.12	62.01	16.23	4.64	54.40	1.01	6.25	0.14	38.20

Note: M: moisture; VM: volatile matter; FC: fixed carbon; A: ash; a.r.: as-received basis; d.a.f.: dry ash-free basis



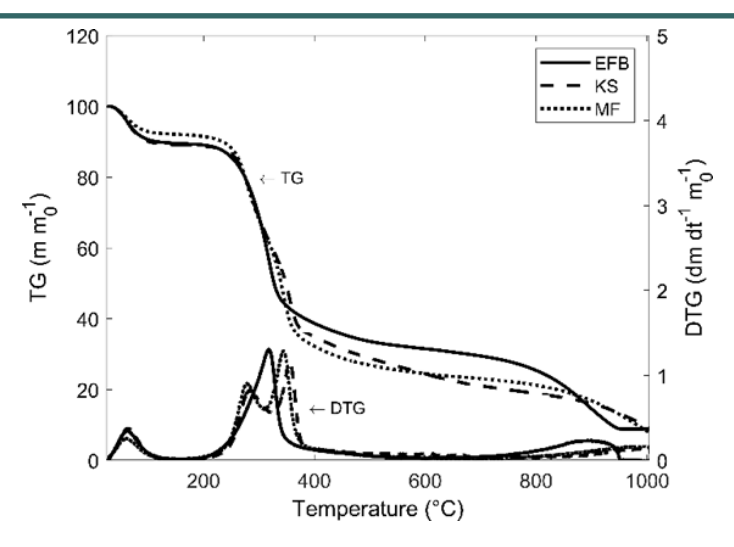


Figure 2. Thermogravimetric curves of oil palm solid waste.

microwave. The flask was then allowed to cool to room temperature for roughly 10 min before taken out from the microwave to remove the obtained char. The pyrolysed raw materials were individual and binary mixtures of oil palm solid waste types. The individual oil palm solid waste types were EFBs, KSs, and MFs. The binary mixtures of oil palm solid waste types comprised EFBs and either KS or MF at 50:50 and 80:20 mass ratios. Pyrolysis with a mass ratio of 20:80 was not conducted to reflect the real industrial scenario, where KS and MF are utilised as solid fuels in steam power plants.

2.4. Liquid Smoke Analysis

The liquid products were collected from the twoneck round-bottom flask and centrifuged using a Ruicheng MC6000 at 6000 rpm to separate the light and heavy phases. The light phase (the water-rich liquid) is the liquid smoke. The heavy phase contains carcinogenic materials unsuitable for human consumption, such as polycyclic aromatic hydrocarbons. The liquid smoke underwent analysis for its chemical compositions and antioxidant capacities. Chemical compounds typically present in liquid smoke, such as phenolic compounds, furanic compounds, carbonyl-containing compounds, and carboxylic acids, were identified using an Agilent 7890B Gas Chromatograph. The antioxidant capacity was evaluated through the 1,1diphenyl-2-picrylhydrazyl (DPPH) assay, where a UV-Vis spectrophotometer measured the color change of the DPPH-treated liquid smoke due to DPPH neutralization. The results were expressed as EC50, indicating the antioxidant concentration

required to reduce DPPH absorbance by 50%. The pH level was measured using a Hanna Instrument HI981030 pH meter.

The chemical compositions of liquid smoke were analysed using Gas chromatography-mass spectrometry (GC-MS) based on a previously reported method [35], with some modifications. To prepare the sample, 1 mL of liquid smoke was with mL of analytical-grade combined 2 dichloromethane, sourced from Sigma-Aldrich. The mixture underwent sonication for about 5 min to ensure the separation into two distinct layers: an upper aqueous layer and a lower dichloromethane layer. A 1 mL portion of the lower layer was then diluted with additional analytical-grade dichloromethane to create a 5-mL solution suitable for GC-MS injection. The analysis was performed using an Agilent 7890B gas chromatograph paired with a 5977B mass spectrometer and fitted with an HP-5MS UI column (30 m \times 250 μ m \times 0.25 μ m). A 1 µl sample was injected at a split ratio of 10:1, with the injector temperature set to 270 °C. The oven temperature was programmed to start at 40 °C (held for 5 min), increase to 100 °C at a rate of 5°C/ min, then rise to 280 °C at 4 °C/min, where it was held for 3 minutes. Helium served as the carrier gas at a flow rate of 1.2 mL/min. Mass spectra were obtained using electron ionization at 70 eV, covering a range of 50-600 amu. Compound identification was achieved by comparing mass spectra with entries in the NIST Research Library and prior studies [35]-[37]. The relative abundance of each compound was determined based on the peak areas in the total ion chromatogram (TIC).



The antioxidant activity was assessed using a method outlined in a previous study [38]. A UV-Vis spectrophotometer was used to monitor the colour change in a liquid smoke solution treated with DPPH, indicating the neutralisation of DPPH radicals. To prepare the DPPH solution, 4 mg of DPPH crystals were dissolved in methanol to create a 40-ppm solution, which was stored in a cold, dark environment to maintain its stability. The liquid smoke sample was dissolved in dimethyl sulfoxide (DMSO) and sonicated for 5 min to ensure uniformity. After preparation, 3 mL of the DPPH solution was combined with 1.5 mL of the liquid smoke solution. The mixture was gently agitated and stored in a cold, dark place for 10 min. Its absorbance was then measured at 518 nm using a UV-Vis spectrophotometer, with each sample tested in triplicate. A blank sample, consisting of 1.5 mL of pure DMSO, was also analysed. The EC₅₀ value was calculated by determining the percentage difference in absorbance between the mixture and the blank sample.

3. RESULTS AND DISCUSSIONS

3.1. Raw Material Characterisation

The results of both proximate and ultimate analyses are presented in Table 3. These findings indicate that the composition of all oil palm solid waste types closely resembles that of softwood and hardwood, which are traditionally used as raw materials for liquid smoke production [39]. The key distinction lies in the higher ash content found in oil

palm waste, attributed to elevated levels of silicon potassium. These elements accumulate throughout the oil palm's lifespan to mitigate physical stress and fulfil nutritional requirements Furthermore, the ultimate analysis [40][41]. revealed that all types of oil palm solid waste share elemental composition, similar primarily consisting of carbon (C) and oxygen (O). This is due to the predominance of lignin and oxygen-rich polysaccharides, namely cellulose hemicellulose, in the biomass [42].

TGA results, illustrated in Figure 2, show that the mass loss profiles of EFBs, KSs, and MFs are broadly similar, likely reflecting their comparable compositions as outlined in Table 3. According to the thermogravimetric curves (Figure 2), up to approximately 250 °C, the materials exhibited around 10% mass loss, primarily due to moisture evaporation. Rapid devolatilisation between 250 and 350 °C, resulting in a mass loss of 60%. During approximately the rapid devolatilisation of EFBs, a single mass loss peak was observed in the DTG curves, likely indicating the simultaneous decomposition of hemicellulose and cellulose [43]. In contrast, the differential thermogravimetry (DTG) curves for KSs and MFs displayed smaller peaks preceding the main peak, suggesting sequential decomposition—first hemicellulose, followed by cellulose [44]. Beyond 350 °C, the rate of devolatilisation slowed markedly, likely due to the gradual decomposition of lignin across a broader temperature range [43].

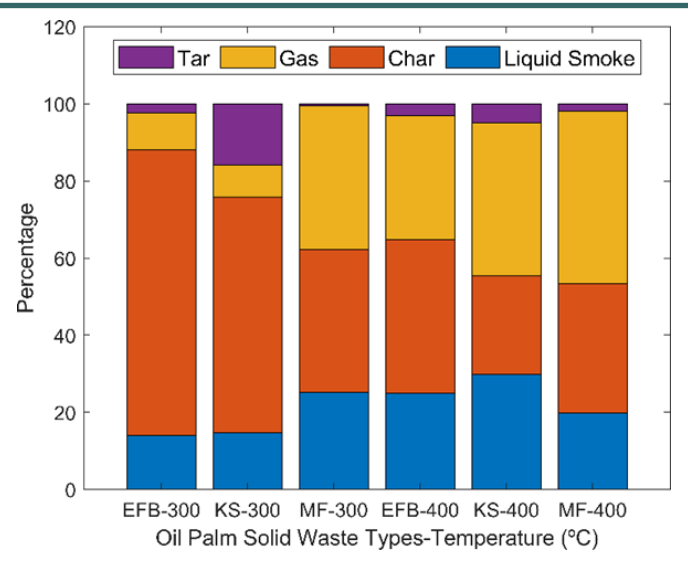


Figure 3. Pyrolytic yield percentage of individual solid waste type.

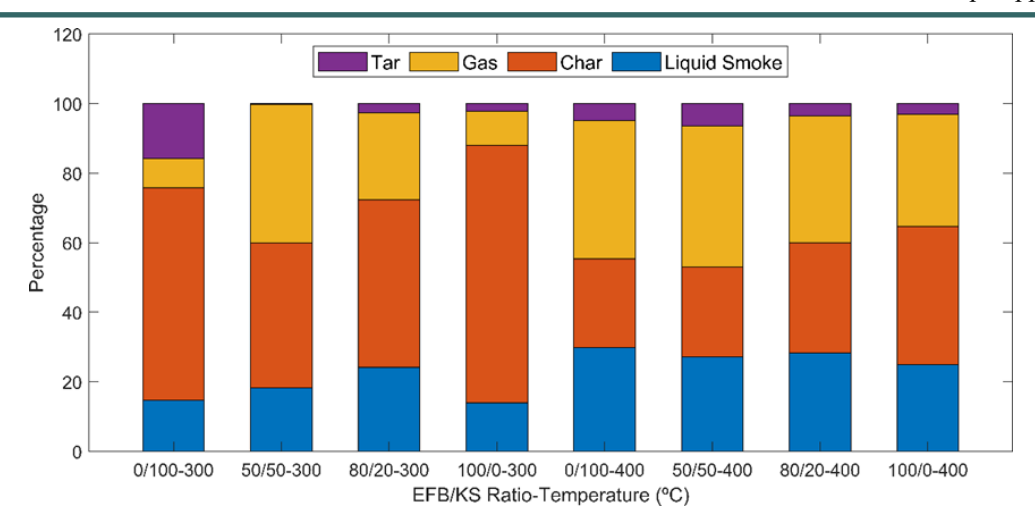


Figure 4. Pyrolytic yield percentage of binary solid waste type mixtures of EFBs and KSs (p < 0.05 for temperatures and p > 0.05 for binary compositions).

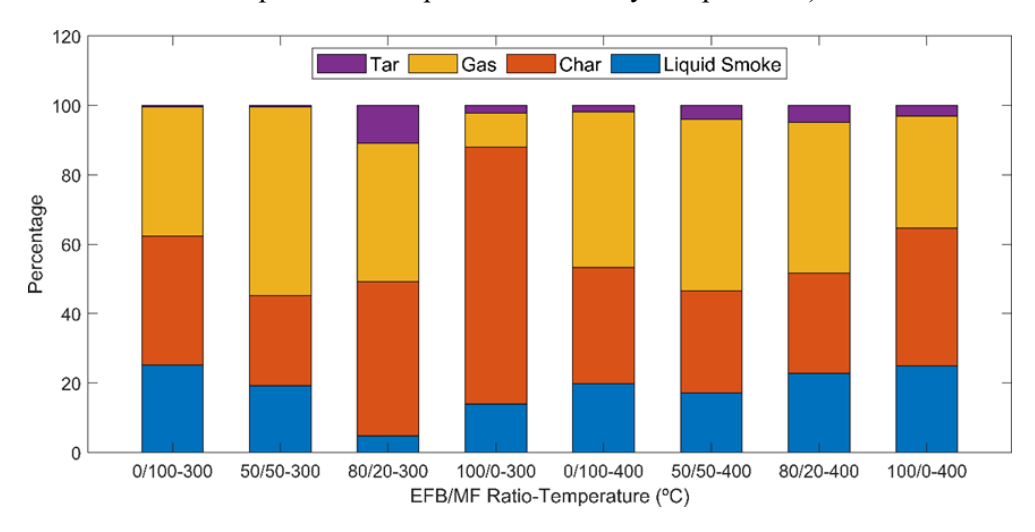


Figure 5. Pyrolytic yield percentage of binary solid waste type mixtures of EFBs and MFs (p > 0.05 for temperatures and p > 0.05 for binary compositions).

3.2. Liquid Smoke Yields of Individual Oil Palm Solid Waste Pyrolysis

The pyrolysis of each oil palm waste type was initially conducted to determine the individual yields of liquid smoke, as shown in Figure 3. For both EFBs and KSs, liquid smoke yields increased significantly by more than 10% when the temperature was raised from 300 to 400 °C. This improvement is attributed to the higher energy input at elevated temperatures, which facilitates faster chemical bond cleavage and the reformation of condensable gas compounds [45][46]. In contrast, MF pyrolysis yielded less liquid smoke at 400 °C than at 300 °C. This finding diverges from previous studies on conventional pyrolysis of MFs, which reported increasing yields with temperature up to a peak, followed by a decline beyond 550 °C due to

extensive cracking and the formation of non-condensable gases [47][48]. The observed yield peak in this study likely occurred at a lower temperature, possibly due to the rapid heating characteristic of microwave-assisted pyrolysis.

3.3. Liquid Smoke Yields of EFB and KS Copyrolysis

The results of co-pyrolysis of EFBs and KSs at 300 and 400 °C are presented in Figure 4. At 300 °C, liquid smoke yields gradually increased from approximately 15% to 25% as the proportion of EFBs rose from 0% to 80%. This increase is likely due to the higher holocellulose content in EFBs which decomposes between 200 and 300 °C into condensable gases [49]. KSs contains a higher ratio of guaiacyl to syringyl units compared to EFBs, and



its degradation is more challenging due to the greater prevalence of C-C bonds in guaiacyl structures [50]. However, when KSs were entirely absent from the feedstock, yields dropped sharply to around 15%. The low guaiacyl content in pure EFBs may have reduced carbocation formation, which is essential for promoting C-O bond cleavage in syringyl units. This, in turn, likely decreased the production of liquid products and increased the formation of solid carbon residues [51]. At 400 °C, liquid smoke yields showed minor fluctuations, with the highest yield at approximately 30% observed in pure KS pyrolysis, and the lowest at around 25% in pure EFB pyrolysis. These variations were considered negligible, as holocellulose was fully decomposed at this temperature, and lignin degradation dominated the reaction, occurring more slowly in KSs due to its structural characteristics [52]. Overall, yields were higher at 400 °C than at 300 °C, indicating that more intensive degradation of both holocellulose and lignin occurs at elevated temperatures.

3.4. Liquid Smoke Yields of EFB and MF Copyrolysis

Figure 5 presents the distribution of pyrolysis products from MAP of oil palm solid waste mixtures consisting of EFBs and MFs at 300 and 400 °C. A prominent trend observed at 300 °C is the progressive decline in liquid smoke yield as MF mass fraction decreases from 100% to 20%, reaching a minimum at the 80:20 EFB-to-MF ratio at around 4.8%. Interestingly, the liquid smoke

yield increased again when EFBs were used alone, reaching approximately 15%. At 400 °C, a similar non-proportional trend is observed, though the minimum liquid smoke yield shifts to the 50:50 blend, again followed by an increase with higher EFB content. This atypical decrease in liquid smoke yield with the introduction of EFBs at 300 °C contradicts general expectations of co-pyrolysis synergy, which often enhances liquid product formation due to complementary decomposition behaviours or synergistic reactions between feedstock components [53]. One possible explanation relates to the inherent properties of MF lignin, which consists predominantly of guaiacyl units (60–75%) with lesser amounts of syringyl and p-hydroxyphenyl structures [54]. Guaiacyl units are more prone to forming stable carbocations during pyrolysis, which can facilitate repolymerisation or char formation rather than depolymerisation into volatile phenolics [55]. This may explain the high liquid smoke yield in pure MF pyrolysis at 300 °C (~25%), where these reactions were optimised, but also the suppression of liquid smoke yield in EFBrich blends where MF lignin was present but potentially destabilised by the co-feed.

Furthermore, from a heat and mass transfer perspective, EFBs and MFs differ markedly in fibre structure and thermal behaviour. As shown in the TGA result (Figure 2), MFs decomposed more readily at lower temperatures compared to EFBs, which contained more hemicellulose and cellulose. The introduction of EFBs might have lowered the average reactivity of the mixture at 300 °C,

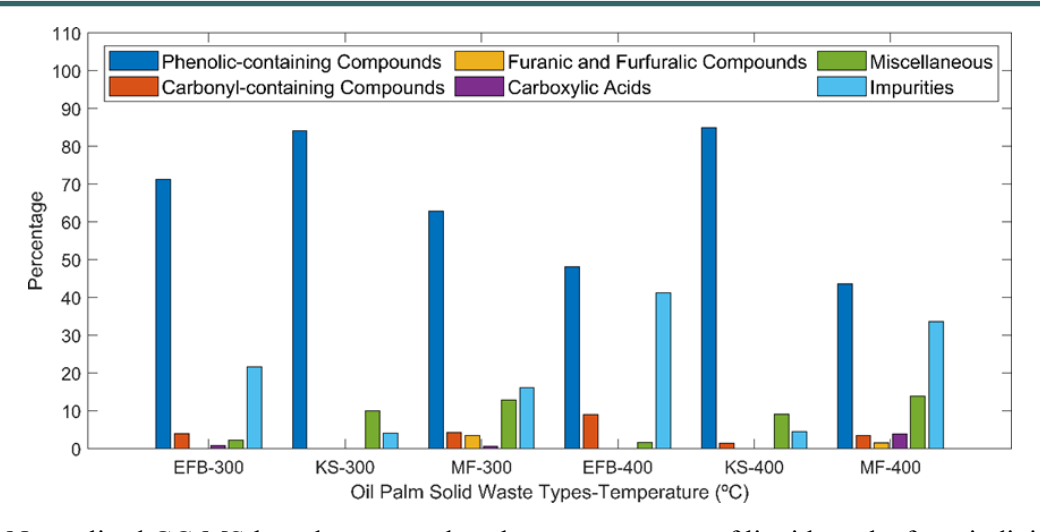


Figure 6. Normalised GC-MS-based compound peak area percentage of liquid smoke from individual solid waste type pyrolysis.

E				Norm	alised Percer	Normalised Percentage of Area		
a	Chemical Compound	EFB	KS	MF	MIX-A	MIX-B	MIX-C	MIX-D
P20	Phenol	54.05	63.28	37.19	57.62	53.61	35.29	35.46
P23	Phenol, 2-methyl-	ND	2.67	1.63	2.88	3.42	ND	2.74
P26	Phenol, 3-methyl-	ND	ND	ND	ND	ND	1.93	ND
P19	p-Cresol	ND	3.54	3.01	3.73	4.43	ND	2.91
P22	Phenol, 2-methoxy	6.33	4.02	4.25	4.27	5.92	5.18	5.39
P25	Phenol, 3,5-dimethyl-	ND	0.64	ND	ND	ND	ND	ND
P13	Creosol	ND	1.29	1.05	0.91	ND	0.77	0.73
P12	Catechol	ND	3.14	4.54	2.93	2.29	3.60	2.60
P2	1,2-Benzenediol, 3-methoxy-	0.89	ND	ND	1.08	1.51	1.87	1.53
P3	1,2-Benzenediol, 3-methyl-	ND	ND	ND	1.33	1.41	1.14	1.64
P4	1,2-Benzenediol, 4-methyl-	ND	1.41	1.64	1.33	ND	1.17	1.24
P21	Phenol, 2,6-dimethoxy-	8.06	3.45	4.85	4.08	6.47	8.43	7.65
P16	Ethyl p-hydroxybenzoate	ND	ND	0.67	0.58	ND	0.46	0.76
P28	Vanillin	ND	ND	69.0	ND	ND	0.74	0.42
P8	3,5-Dimethoxy-4-hydroxytoluene	0.59	92.0	1.27	0.77	ND	1.04	0.79
P14	Ethanone, 1-(3-hydroxy-4-methoxyphenyl)-	ND	ND	ND	ND	ND	0.41	ND
P7	2,4-Di-tert-butylphenol	0.61	ND	ND	ND	ND	ND	ND
P9	5-tert-Butylpyrogallol	0.75	ND	ND	ND	ND	0.45	ND
P5	2 Propanone, 1-(4-hydroxy-3-methoxyphenyl)-	ND	ND	0.75	ND	ND	0.87	89.0
P10	Benzaldehyde, 4-hydroxy-3,5-dimethoxy	ND	ND	0.52	ND	ND	0.56	0.41
P15	Ethanone, 1-(4-hydroxy-3,5-dimethoxyphenyl)-	ND	ND	ND	ND	ND	0.65	0.41
P27	Syringylacetone	ND	ND	0.75	ND	ND	0.99	0.81
Total (Total (Phenolic Compounds)	71.30	84.20	62.80	81.50	79.10	09.59	66.20
CC4	2-Cyclopeten-1-one, 2-methyl-	ND	ND	1.03	ND	1.94	1.43	2.59



Table 4. Cont.

É				Norma	lised Percen	Normalised Percentage of Area		
A	Cnemical Compound	EFB	KS	MF	MIX-A	MIX-B	MIX-C	MIX-D
CC7	2-Cyclopeten-1-one, 3-hydroxy-2-methyl-	2.49	ND	3.17	2.93	4.28	4.23	4.34
CC3	2-Cyclopeten-1-one, 2,3-dimethyl-	ND	ND	ND	ND	ND	0.46	0.83
CC5	2-Cyclopeten-1-one, 3,4,5-trimethyl	0.56	ND	ND	ND	ND	ND	ND
9 2 2	2-Cyclopeten-1-one, 3-ethyl-2-hydroxy	0.93	ND	ND	ND	ND	0.85	1.01
Total (Total (Carbonyl-containing Compounds)	3.98	0	4.20	2.93	6.22	6.97	8.77
FF1	2(5H)-Furanone	ND	ND	2.62	ND	ND	ND	N
FF2	2-Furancarboxaldehyde, 5-methyl	ND	ND	0.81	ND	ND	0.44	ND
Total (Total (Furanic and Furfuralic Compounds)	0	0	3.43	0	0	0.44	0
CA2	Methyl hexadecanoate	ND	ND	ND	1.19	ND	ND	ND
CA3	n-Hexadecanoic acid	0.88	ND	09.0	1.01	ND	0.58	N
CA1	Methyl 9(Z)-Octadecenoate	ND	ND	ND	1.05	ND	ND	N
Total (Total (Carboxylic Acids)	0.88	0	09.0	3.25	0	0.58	0
N3	1H-Pyrazole, 1,5-dimethyl-	ND	9.95	12.27	ND	ND	ND	ND
X 4	1H-Pyrazole, 4,5-dihydro-3-methyl-1-propyl-	1.35	ND	ND	ND	ND	ND	N
N9	Cyclopentane, ethylidene-	ND	ND	ND	1.03	ND	ND	ND
\overline{z}	1,3-Dimethyl-1-cyclohexene	ND	ND	ND	ND	ND	ND	0.44
N2	1-ethoxy-2,4-hexadiene	0.89	ND	0.58	ND	ND	ND	ND
N Z	Benzene, 1,2,3-trimethoxy-5-methyl-	ND	ND	ND	ND	ND	ND	0.47
Total (Total (Miscellaneous)	2.24	9.95	12.9	1.03	0	0	0.91
dwl	Impurities	21.63	4.07	16.11	11.28	14.73	26.46	24.16
Total (Total (Impurities)	21.63	4.07	16.11	11.28	14.73	26.46	24.16
Note: ML	Note: MIX-A: EFB 50% KS 50%; MIX-B: EFB 80% KS 20%; MIX-C: EFB 50% MF 50%; MIX-C: EFB 80% MF 20%; ND: Not detected	: EFB 80% MF	0%: ND: Not	letected				

Table 5. GC-MS analysis results of entire chemical compounds of liquid smoke produced via microwave-assisted pyrolysis of oil palm solid waste at 400 °C.

E				Norma	lised Percen	Normalised Percentage of Area		
M	Chemical Compound	EFB	KS	MF	MIX-A	MIX-B	MIX-C	MIX-D
P20	Phenol	25.49	65.91	24.99	46.73	44.82	29.80	25.45
P23	Phenol, 2-methyl-	3.14	2.22	1.25	3.44	2.59	2.30	2.48
P19	p-Cresol	3.77	3.14	1.95	4.59	3.15	3.30	3.08
P22	Phenol, 2-methoxy	4.49	4.20	4.60	3.92	4.99	4.66	5.05
P13	Creosol	0.73	1.12	1.32	1.02	0.67	0.85	0.91
P12	Catechol	ND	3.53	ND	1.56	2.40	ND	1.20
P2	1,2-Benzenediol, 3-methoxy-	ND	ND	ND	ND	2.92	ND	ND
P4	1,2-Benzenediol, 4-methyl-	ND	1.22	ND	1.05	0.82	ND	0.82
P6	2,3-Dimethoxyphenol	5.02	2.81	ND	4.69	ND	ND	7.21
P21	Phenol, 2,6-dimethoxy-	ND	ND	5.42	ND	6.40	5.32	ND
P16	Ethyl p-hydroxybenzoate	ND	ND	ND	0.63	ND	ND	ND
P8	3,5-Dimethoxy-4-hydroxytoluene	0.73	0.74	1.49	86.0	0.81	0.90	1.28
P18	Methylparaben	ND	ND	0.53	ND	ND	ND	ND
P24	Phenol, 3,5-bis(1,1-dimethylethyl)-	ND	ND	ND	ND	0.55	ND	ND
P111	Butylated hydroxytoluene	2.43	ND	ND	ND	ND	66.9	ND
P17	Guaiacol, 4-butyl-	ND	ND	ND	ND	ND	ND	ND
P5	2-Propanone, 1-(4-hydroxy-3-methoxyphenyl)	0.63	ND	0.99	89.0	0.62	69.0	0.94
P1	(E)-4-(3-Hydroxyprop-1-en-1-y1)-2-methoxyphenol	0.88	ND	ND	ND	ND	ND	ND
P27	Syringylacetone	0.81	ND	1.06	ND	0.53	0.82	1.30
Total (Total (Phenolic Compounds)	48.10	84.90	43.60	69.30	71.30	55.60	49.70
CC4	2-Cyclopenten-1-one, 2-methyl-	2.81	ND	92.0	1.07	1.55	ND	2.06
CC8	2-Cyclopenten-1-one, 3-methyl-	ND	ND	ND	0.55	ND	ND	ND
CC7	2-Cyclopenten-1-one,3-hydroxy-2-methyl-	2.67	1.46	2.13	2.49	3.69	2.02	3.67
CC3	2-Cyclopenten-1-one, 2,3-dimethyl-	0.76	ND	ND	ND	0.57	0.62	ND
3	2-Cyclopenich-1-010, 2,5-dimediyi-	00	QVI	QVI	QVI	7.5.0	70.0	

Table 5. Cont.

£				Norma	lised Percen	Normalised Percentage of Area		
an I	Cnemical Compound	EFB	KS	MF	MIX-A	MIX-B	MIX-C	MIX-D
9 2 2	2-Cyclopenten-1-one, 3-ethyl-2-hydroxy-	ND	ND	0.65	0.50	0.71	ND	96.0
CC1	1,3-Cyclopentanedione, 2,4-dimethyl-	0.63	S	ND	ND	ND	0.65	ND
CC2	2,6-Di-tert-butyl-4-hydroxy-4-methylcyclohexa-2,5-dien-1-one	ND	ND	ND	ND	ND	99.0	ND
CC9	Methyl hexadecanoate	1.65	ND	ND	ND	ND	ND	ND
CC10	Methyl stearate	0.54	ND	ND	ND	N	N	ND
Total (Total (Carbonyl-containing Compounds)	90.6	1.46	3.54	4.61	6.52	3.95	69.9
FF2	2-Furancarboxaldehyde, 5-methyl-	N	ND	1.53	ND	N	N	ND
Total (Total (Furanic and Furfuralic Compounds)	0	0	1.53	0	0	0	0
CA3	n-Hexadecanoic acid	ND	ND	2.18	1.36	0.75	ND	5.10
CA4	Octadecanoic acid	ND	ND	1.67	1.40	ND	ND	6.30
Total (Total (Carboxylic Acids)	0	0	3.85	2.76	0.75	0	11.40
9N	4-Cyanoimidazole	1.55	ND	ND	ND	ND	ND	ND
N11	Pyridine, 2-methyl-	N	ND	ND	ND	N	1.57	ND
N5	2-Aminopyridine	ND	ND	ND	ND	ND	98.0	ND
N3	1 <i>H</i> -Pyrazole, 1,5-dimethyl-	ND	60.6	13.34	ND	ND	ND	ND
N	Benzene, 1,2,3-trimethoxy-5-methyl-	ND	ND	0.53	ND	ND	ND	ND
N10	Cyclotetrasiloxane, octamethyl-	ND	ND	ND	ND	ND	ND	1.62
8N	Cyclic octaatomic sulfur	ND	S	ND	ND	ND	ND	2.36
Total (Total (Miscellaneous)	1.55	60.6	13.87	0	0	2.43	3.98
dwl	Impurities	41.26	4.56	33.59	23.36	21.46	37.99	28.22
Total (Total (Impurities)	41.26	4.56	33.59	23.36	21.46	37.99	28.22
Note - MT	Note: MIX.A. FEB 50% KS 50%: MIX.B. FEB 80% KS 20%: MIX.C. FEB 50% ME 50%	: MIX C : FFB 80% ME 20%: ND: Not detected	2007. MID. Mot	2400400				

Note: MIX-A: EFB 50% KS 50%; MIX-B: EFB 80% KS 20%; MIX-C: EFB 50% MF 50%; MIX-C: EFB 80% MF 20%; ND: Not detected

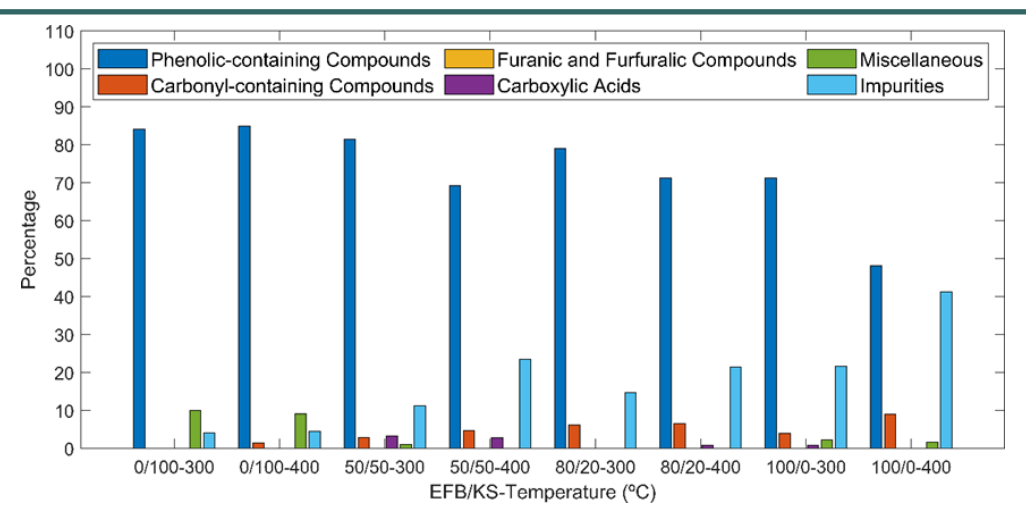


Figure 7. Normalised GC-MS-based compound peak area percentage of liquid smoke from pyrolysis of binary solid waste type mixtures of EFBs and KSs (p > 0.05 for temperature effect and p < 0.05 for binary composition effect on normalised phenolic compound peak area percentage).

fully insufficient volatilise MF-derived to compounds before secondary reactions dominated. This is further complicated by potential differences in microwave absorption characteristics; although EFBs has a higher dielectric constant and loss factor than MFs, resulting in stronger microwave coupling [56], this may have also promoted localised overheating that accelerated tar or char formation, particularly when MF was present in minor proportion. A particularly noteworthy observation is that MAP of pure EFBs yielded more liquid smoke than the mixture of EFBs and MFs with 80:20 ratio at 300 °C. While MFs alone were more reactive and yielded higher yields of liquid smoke, their behaviour in the blend appears non-proportional. Hypothetically, the small fraction of MF lignin in the mixture with 80:20 ratio might have engaged in inhibitory interactions with the EFB matrix, via possibly cross-linking or incomplete devolatilisation, leading to enhanced char formation rather than volatile release. Meanwhile, pure EFBs underwent more uniform microwave heating due to its stronger dielectric properties, resulting in consistent devolatilisation of cellulose hemicellulose fractions and comparatively milder secondary reactions. As a result, EFBs produced liquid smoke with yield at around 15%, whereas the mixture of EFBs and MFs produced significantly less due to both chemical inhibition and thermal heterogeneity within the mixture. The increase in liquid smoke yield with increasing EFB content at 400 °C suggests that higher energy input overcame

this inhibitory effect, consistent with previous findings showing that EFBs released more volatiles at elevated temperatures due to enhanced cellulose and hemicellulose breakdown [57]. This also aligns with the general trend in biomass pyrolysis, where increasing temperature typically shifts product distribution toward more condensable vapours and gas, up to a certain threshold [58].

3.5. Distribution of Chemical Compound Groups in Liquid Smoke from Individual Oil Palm Solid Waste Type Pyrolysis

Figure 6 presents the GC-MS-measured normalised cumulative peak areas of major chemical groups found in liquid smoke produced from the pyrolysis of individual oil palm solid waste types. These groups include phenolic compounds, carbonyl-containing compounds, furanic and furfuralic compounds, carboxylic acids, miscellaneous compounds, and impurities.

In EFB pyrolysis at 300 °C, approximately 70% of the organic compounds in the liquid smoke were phenolic, with impurities accounting for around 20%, and all other compounds present only in trace amounts (less than 5%). This high proportion of phenolic compounds was unexpected, given that EFBs contain over 80% holocellulose [59]. As the temperature approached 300 °C, cellulose was converted into oligosaccharides due to the cleavage of most β -(1 \rightarrow 4)-glycosidic bonds [60]. These oligosaccharides then underwent three degradation pathways: dehydration, reconstruction, and



fragmentation. Dehydration broke the glycosidic forming monomeric sugars such levoglucosan, levoglucosanone, 1,4:3,6-dianhydroβ-D-glucopyranose, 1,6-anhydro-β-Dand glucofuranose Reconstruction [61][62]. reassembled these monomers into furanic and furfuralic compounds, including furfural, hydroxymethylfurfural, furan, and 2-methylfuran [63]-[65]. Fragmentation cleaved the monomers into light carbonyl-containing compounds such as acetone, acetol, and hydroxyacetaldehyde [66][67]. Despite the high cellulose content in EFBs, cellulose-derived compounds were only present in negligible amounts in the liquid smoke. It is likely that these compounds, in gaseous form, were further degraded into stable non-condensable gases—such as CO, CO2, H2, and H2O—before exiting the pyrolysis system, due to the rapid heating rates induced by microwave treatment. Additional degradation may have occurred just above the solid phase, albeit at slower rates, as microwave radiation has minimal effect on gases due to their low dielectric permittivity [68]. Hemicellulose, which constitutes less than 10% of EFBs, was likely degraded into various compounds at lower temperatures (200–300 °C), owing to its amorphous structure. However, hemicellulosederived compounds were largely absent from the liquid smoke, except for minor traces of carbonylcontaining compounds and carboxylic acids. These may indicate the dominance of O-acetylxylan units in EFB hemicellulose and trace contributions from

oil palm lipids [69]. The scarcity of hemicellulosederived compounds is also likely due to their conversion into non-condensable gases before leaving the solid phase.

As the temperature increased towards 300 °C, lignin began to lose structural integrity and underwent depolymerisation via cleavage of C-O and C=O bonds. This process typically yields methoxyphenols as the dominant products. However, in this case, phenol normally formed through demethylation and demethoxylation of methoxyphenols at temperatures above 350 °C was the major compounds in the liquid smoke, accounting for over 50% of the normalised peak area (see Table 4) [70]. The significant presence of phenol at 300 °C suggests that microwave irradiation may have facilitated demethylation and demethoxylation at lower temperatures [71]. Unlike holocellulose-derived compounds, phenol was retained in high quantities, likely due to the thermal stability of the benzene ring structure during pyrolysis [72]. Approximately 20% of the organic compounds in the liquid smoke were classified as comprising numerous unidentified impurities, compounds with very small individual peaks. Although the exact origin of these impurities remains unclear, they are likely aliphatic compounds derived from the phenylpropane side chains released during lignin degradation.

In EFB pyrolysis at 400 °C, the proportion of phenol decreased by approximately 20%, while the percentage of carbonyl-containing compounds

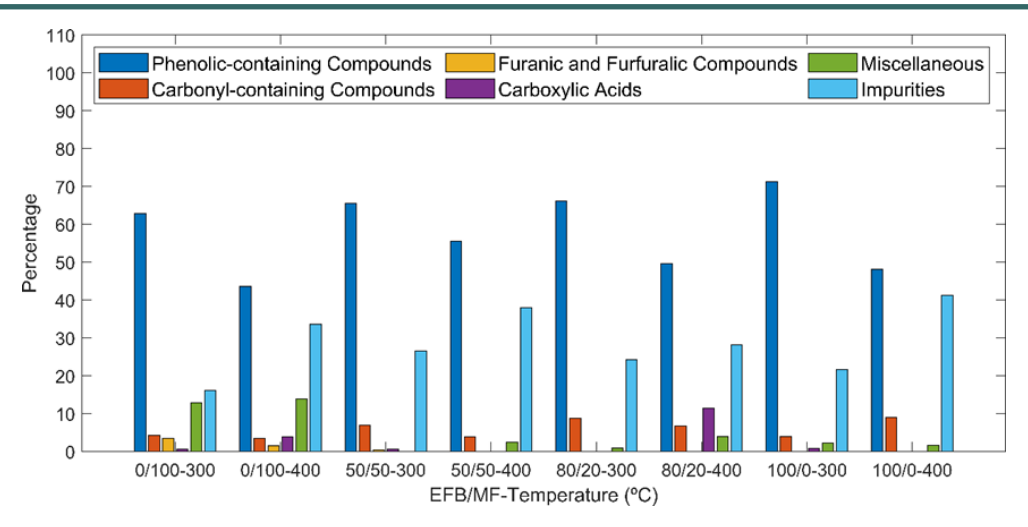


Figure 8. Normalised GC-MS-based compound peak area percentage of liquid smoke from pyrolysis of binary solid waste type mixtures of EFBs and MFs (p < 0.05 for temperature effect and p > 0.05 for binary composition effect on normalised phenolic compound peak area percentage).

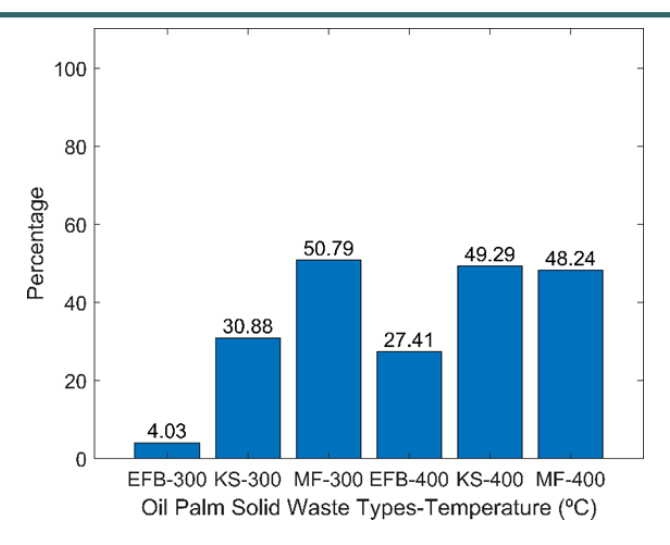


Figure 9. ACs of liquid smoke produced from individual solid waste type MAP.

increased slightly compared to that at 300 °C. The higher concentration of carbonyl-containing compounds in the liquid smoke at 400 °C suggests secondary decomposition of monomeric sugars into compounds, carbonyls, furanic derivatives. The absence of furanic and furfuralic compounds in the final product may be due to their breakdown carbonyl-containing further into compounds at this temperature [73]. Moreover, furan and furfural compounds are more prone to decomposition into non-condensable gases than carbonyl-containing compounds, owing to the weak oxygen bonds in their five-membered aromatic rings [74]. Similarly, a small fraction hemicellulose may have decomposed additional carbonyl-containing compounds at 400° C, contributing to the observed increase. According to Table 5, most of the carbonyl-containing compounds in the liquid smoke from EFB pyrolysis were cyclopentene derivatives. These may have formed either through the cracking of furanic and furfuralic compounds or via alkali-metal-rich ashcatalysed Michael-Aldol condensation, which facilitates the cyclisation of aliphatic carbonyl compounds [75]-[77]. Compared to lignin-derived compounds at 300 °C, those at 400 °C appeared in lower proportions, likely due to reduced thermal stability at higher temperatures. However, as shown in Tables 4 and 5, selectivity towards cresol- and catechol-type compounds was higher at 400 °C. Theoretical formation of cresol compounds involves methyl radical reactions with methoxyphenols, while catechol compounds are formed when hydrogen radicals generated from

carbonyl compound cracking react with phenoxy radicals produced from methoxyphenol interactions with oxygen radicals [78]. Additionally, the proportion of impurities was higher at 400 °C than at 300 °C, possibly indicating an increased release rate of phenylpropane side chains from lignin under more intense thermal conditions.

At both 300 and 400 °C, the liquid smoke produced from KS pyrolysis exhibited remarkably consistent compound selectivity. Regardless of temperature, the proportion of phenolic compounds remained stable at approximately 85%, while miscellaneous compounds and impurities accounted for less than 10%. This consistency is likely due to the high content of KS lignin serving as the primary source of phenolic compounds [79]. As shown in Tables 4 and 5, the relative proportions of phenol and methoxyphenols, cresol, and catechol were also similar across both temperatures. The rapid heating rates achieved in KSs, facilitated by its high porosity and enhanced by microwave treatment, may have contributed to the stable phenolic yield and distribution. enabling efficient lignin conversion into phenolic compounds [80]. 10% Approximately of the miscellaneous compounds consisted of methyl pyrazole, which likely originated from protein content in KSs [81]. At elevated temperatures, these proteins may have undergone depolymerisation and, upon passing through the condenser, cyclised into pyrazole [82]. An alternative mechanism for pyrazole formation involves the Maillard reaction between amino acids produced from protein degradation and carbonylcontaining compounds derived from holocellulose



breakdown, followed by Amadori rearrangement [83].

In MF pyrolysis, phenolic compounds were also dominant at both temperatures, while holocellulosederived products appeared only in trace amounts. At 300 °C, phenolic compounds accounted for approximately 63% of the organic compounds in the liquid smoke, but this proportion dropped to around 44% at 400 °C. Similar to EFB pyrolysis, the phenolic compounds in MFs may have been degraded at higher temperatures as they exited the biomass during pyrolysis. The higher percentage of miscellaneous compounds, particularly methyl pyrazole, in MF pyrolysis compared to KS pyrolysis at both temperatures may be attributed to the breakdown of a relatively large quantity of nitrogen-rich enzymes in MFs. These enzymes play a crucial role in catalysing metabolic reactions during palm oil formation and contribute to capacity of MFs to store up to 80% of its dry mass as oil [84]. The proportion of impurities in MF pyrolysis was below 20% at 300 °C but rose significantly to approximately 35% at 400 °C, coinciding with a nearly 20% reduction in phenolic content. This trend, similar to that observed in EFB pyrolysis, suggests that elevated temperatures may partially promote the conversion of phenolic compounds into impurities.

3.6. Distribution of Chemical Compound Groups in Liquid Smoke from EFB and KS Co-pyrolysis

Figure 7 presents the normalised GC-MS-based compound peak area percentages of liquid smoke

obtained from the pyrolysis of binary mixtures of EFB and KS, with EFB-to-KS ratios of 0:100, 50:50, 80:20, and 100:0, at both 300 and 400 °C. As the EFB-to-KS ratio increased, the percentage of phenolic compounds decreased, reflecting the reduced mass of KS, which is rich in lignin, the primary source of phenolic compounds. At 300 °C, methoxyphenols such as 2-methoxyphenol and 2,6dimethoxyphenol were present in relatively significant amounts, and their percentages declined as the EFB-to-KS ratio decreased (Table 4). However, at 400 °C, methoxyphenol levels showed no clear trend with changing EFB-to-KS ratios. In contrast, phenol percentages were consistently higher at 300 °C than at 400 °C and increased steadily with rising EFB content. As previously discussed, the high heating rates generated by microwave treatment may have enhanced the conversion of guaiacyl units as the dominant component in KS lignin into catechol- and cresoltype compounds and phenol [85]. Given the similar proportions of catechol, cresol, methoxyphenols at both temperatures, the lower phenol content at 400 °C compared to 300 °C may suggest that more lignin was degraded into impurities and non-condensable gases at the higher temperature. The percentage of carbonyl-containing compounds increased as EFBs became dominant component in the mixture, indicating that holocellulose as the abundant component in EFBs was the primary source of these compounds. Pyrolysis of mixtures with higher EFB-to-KS ratios produced liquid smoke with lower phenolic content

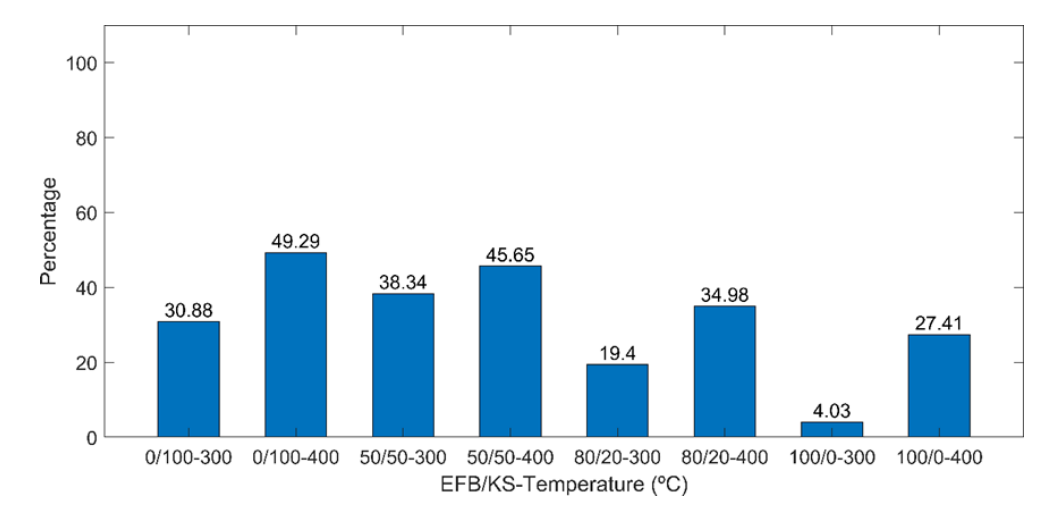


Figure 10. ACs of liquid smoke produced from MAP of binary solid waste type mixtures of EFBs and KSs (p > 0.05) for temperatures and p < 0.05 for binary compositions).

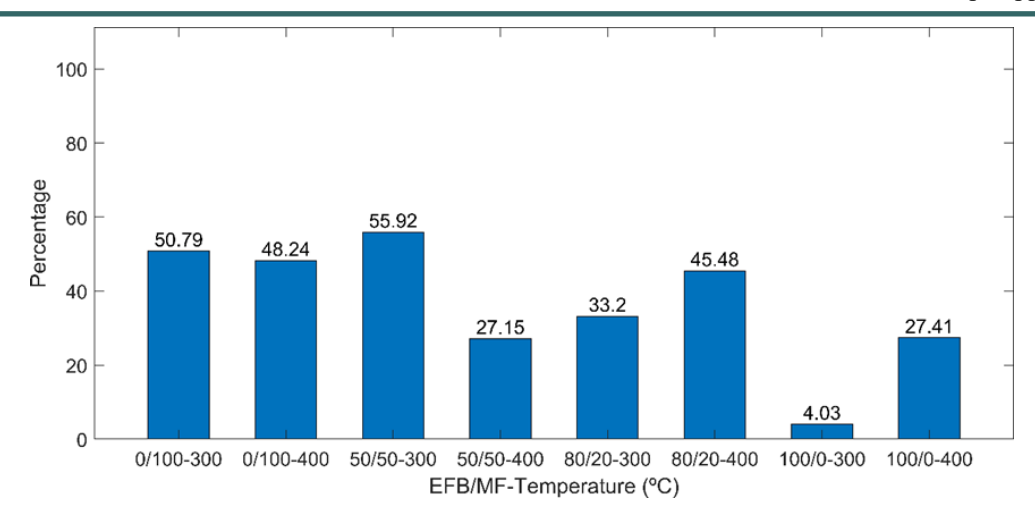


Figure 11. ACs of liquid smoke produced from MAP of binary solid waste type mixtures of EFBs and MFs (p < 0.05 for temperatures and p > 0.05 for binary compositions).

and higher impurity levels compared to mixtures with lower EFB-to-KS ratios. This finding suggests that some impurities may originate from non-lignin, holocellulose-derived compounds, as higher EFB-to-KS ratios correspond to greater holocellulose content in the feedstock.

3.7. Distribution of Chemical Compound Groups in Liquid Smoke from EFB and MF Co-pyrolysis

Figure 8 displays the normalised GC-MS-based compound peak area percentages of liquid smoke obtained from the pyrolysis of binary mixtures of EFBs and MFs, with EFB-to-MF ratios of 0:100, 50:50, 80:20, and 100:0, at both 300 and 400 °C. At 300 °C, a decrease in the EFB-to-MF ratio led to a reduction in the percentage of phenolic compounds, possibly due to the high concentration of guaiacyl units in MF, which may have promoted char formation. At 400 °C, however, no clear trend in phenolic compound percentages was observed. Overall, the proportion of phenolic compounds declined as the pyrolysis temperature increased from 300 to 400 °C, likely due to greater thermal degradation of these compounds at elevated temperatures. Nevertheless, as shown in Table 4, the variability of phenolic compounds such as cresol-type compounds, catechol-type compounds, and methoxyphenols was greater at 400 °C across all blend ratios. Their percentages may have increased with rising EFB-to-MF ratios, suggesting improved selectivity for these compounds at higher temperatures. Compared to the pyrolysis of EFB-KS mixtures, the pyrolysis of EFB-MF mixtures resulted in higher percentages of impurities. This is likely due to the predominance of holocellulose in the EFB–MF feedstock, which may contribute to the formation of non-phenolic, holocellulose-derived impurities.

3.8. Antioxidant Capacities of Liquid Smoke

The antioxidant capacities (ACs) of liquid smoke derived from MAP of oil palm solid waste (Figure 9) exhibit trends consistent with previous studies on pyrolysis-derived bio-oils. For instance, the ACs of liquid smoke from mesocarp fibres MAP at 300 °C (50.79%) align with values reported for yew tree bark pyrolysis liquids (58.76% DPPH scavenging), likely due to its high phenolic content, particularly catechol and syringol derivatives, which are known for their radical scavenging efficacy [86][87]. Notably, increasing the pyrolysis temperature from 300 °C to 400 °C enhanced the ACs of most liquid smoke (e.g., 4.03% to 27.41% for EFB liquid smoke and 30.88% to 49.29% for KS liquid smoke), phenomenon also observed lignocellulosic bio-oils produced at 150-500 °C [88]. This improvement is attributed to the formation of advanced antioxidants such as alkylated phenols (e.g., creosol) and methoxysubstituted derivatives (e.g., 3,5-dimethoxy-4hydroxytoluene), which exhibit superior stability electron-donating capabilities However, MFs showed a marginal decline in ACs (50.79% at 300 °C to 48.24% at 400 °C), likely due to the thermal degradation of potent orthodihydroxy phenols like catechol (4.54% at 300 °C



to ND at 400 °C), despite the increased presence of moderate antioxidants such as 2,6-dimethoxyphenol (4.85% at 300 °C to 5.42% at 400 °C) [91].

The high ACs of KS-derived liquid smoke at 400 °C (49.29%) correlates with its high catechol (3.53%) and phenol (65.91%) content (Tables 4 and 5). Catechol is a strong antioxidant due to its 1,2-diol structure, which facilitates hydrogen atom transfer and radical stabilization [92]. This aligns with studies on spruce wood bio-oil, where catechol-rich fractions demonstrated significantly higher AC than mono-phenolic-dominated samples [93]. Conversely, the lower ACs of EFB-derived liquid smoke (4.03% at 300 °C) reflects its simpler phenolic profile, dominated by phenol (54.05%) with minimal contributions from polyfunctional antioxidants.

Blending EFBs with KSs or MFs introduced nonproportional trends in ACs. For EFB-KS mixtures (Figure 10), the ACs decreased with higher EFB ratios (e.g., 38.34% for 50:50 to 19.4% for 80:20 at 300 °C), mirroring observations in blended biomass pyrolysis, where diluted phenolic reduced concentrations antioxidant efficacy [94]. The exceptional ACs of EFB-KS mixture with ratio of 50:50 (38.34% at 300 °C) may arise from synergistic interactions between 3-methoxy-1,2-(1.08%)benzenediol and catechol (2.93%),compounds known to enhance radical scavenging through redox mediation. Catechol, an orthodihydroxy phenol, exhibits superior radical

scavenging activity due to its ability to donate hydrogen atoms from both hydroxyl groups, forming a stable quinone intermediate. Meanwhile, 3-methoxy-1,2-benzenediol, a methoxy-substituted derivative, enhances this effect by stabilizing radical intermediates through resonance delocalization facilitated by its electron-donating methoxy group. This synergy is mechanistically akin to the cooperative effects observed in natural antioxidant systems, where polyphenols with mixed substitution patterns (e.g., hydroxyl/methoxy) exhibit enhanced activity compared to isolated compounds [95]. For EFB-MF mixtures, the nonproportional ACs trend (Figure 11) suggests an optimal intermediate ratio at 80:20. The sharp ACs decline for EFB-MF with ratio of 50:50 at 400 °C (55.92% to 27.15%) underscores the critical role of catechol degradation, as its complete disappearance offset gains from other antioxidants like creosol (0.91% to 1.02%) [96].

From a chemical perspective, the observed AC trends were driven by three key mechanisms: (i) ortho-dihydroxy phenolic compounds catechol) exhibits high electron delocalisation and capacity; hydrogen-donation (ii) methoxysubstituted phenolic compounds (e.g., 2,6dimethoxyphenol) stabilise radicals through resonance effects; and (iii) alkylated phenolic compounds (e.g., creosol) terminates radical chain reactions via stable phenoxyl intermediate formation. These mechanisms collectively explain

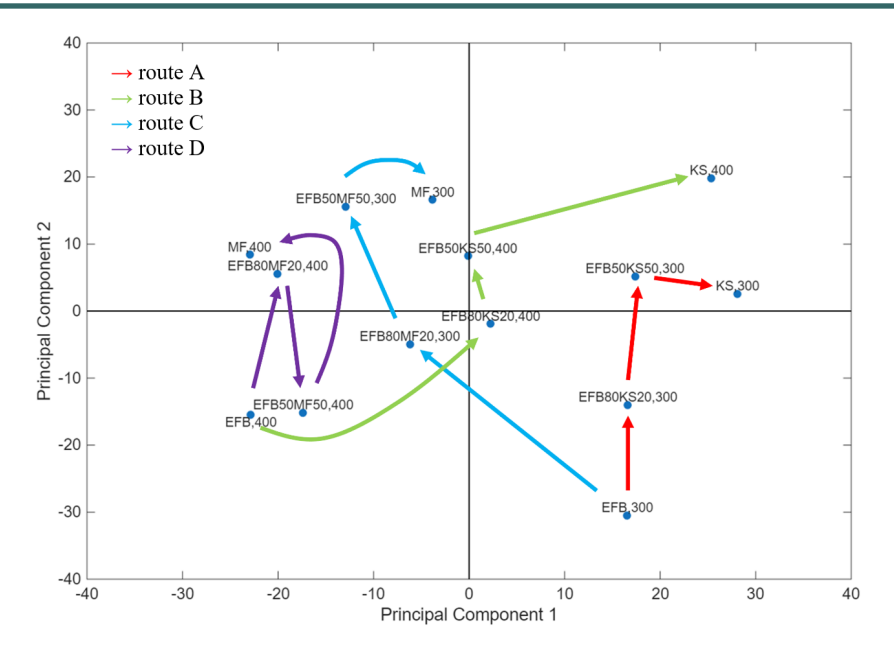


Figure 12. Score plot of PC1 and P2 for GC-MS analysis results.

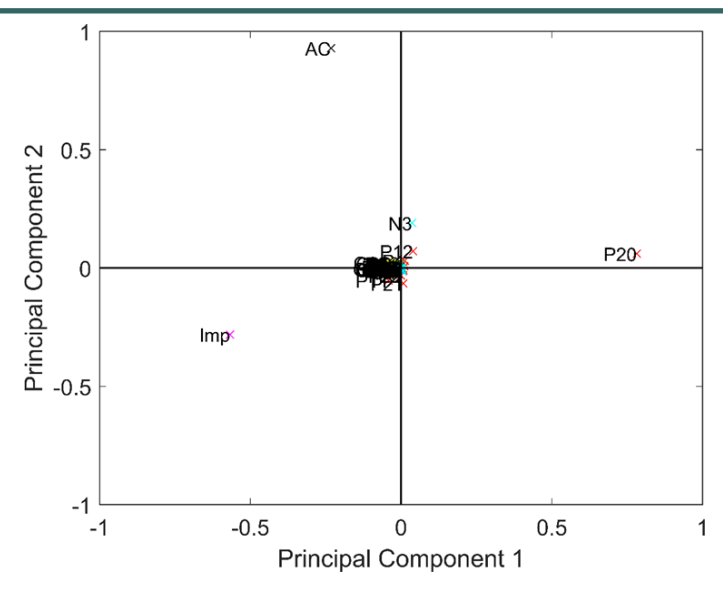


Figure 13. Loading plot of PC1 and PC2 for the results of GC-MS analysis with chemical compound IDs listed in Tables 4 and 5 and the antioxidant capacity.

why liquid smoke with diverse phenolic profiles such as KS-derived (catechol-rich) against EFB-derived (phenol-dominated), show marked differences in AC despite similar pyrolysis conditions.

3.9. Significance of MAP Temperature and Oil Palm Solid Waste Blending Ratio Effects

Statistical significance via linear regression analysis revealed distinct parameter sensitivities across different output metrics in MAP of EFB and KS mixture. MAP temperature emerged as the dominant factor for liquid smoke yield (p = 0.017), consistent with established pyrolysis mechanisms elevated temperatures promote complete biomass decomposition through enhanced cleavage of glycosidic and β -O-4 lignin linkages. However, the non-significant EFB-KS blend ratio effect (p = 0.88) indicates the relative proportions of these feedstocks (50:50 to 80:20) minimally impact total volatile production, likely due to their similar lignocellulosic composition, particularly in lignin content (20–25%). For antioxidant capacity, both temperature (p = 0.039) and blend ratio (p =0.028) showed significant but competing influences. While higher temperatures increased total volatiles, they simultaneously degraded thermolabile antioxidants like catechol, whereas KS -rich blends consistently enhanced activity through greater production of ortho-diphenolic compounds from syringyl-rich lignin. This blenddependent antioxidant production was itself temperature-sensitive, peaking at intermediate conditions. Normalised percentages of phenolic compounds profiles were primarily governed by blend ratio (p = 0.03), reflecting greater KS contribution of methoxyphenols, while temperature showed only marginal significance (p = 0.10) as phenolic degradation at higher temperatures was apparently balanced by new phenolic compounds secondary through repolymerization reactions. These analysis results demonstrate that while temperature controls bulk yield, mixture composition of EFBs and KSs serves as the primary lever for tailoring product functionality, with optimal conditions requiring careful balancing of these competing effects.

The analysis revealed fundamentally different behaviour for EFB-MF blends compared to EFB-KS systems. Neither MAP temperature (p = 0.31) nor blend ratio (p = 0.45) significantly influenced liquid smoke yield, suggesting high hemicellulose content (30-35%) in MFs promotes rapid and consistent devolatilization across the tested conditions. This yield stability occurred despite dramatic temperature effects on phenolic composition (p = 0.0014), indicating decomposition kinetics of MFs are decoupled from speciation. The non-significant product temperature effect on antioxidant capacity (p = 0.92) further highlights this decoupling, contrasting sharply with EFB-KS blends. While EFB-MF ratio



showed marginal significance for antioxidant capacity (p = 0.10), this likely reflects competing processes, e.g., the produced furanic compounds might have contributed to antioxidant activity at certain blend ratios, but their effects were less pronounced than the phenolic-driven activity in KScontaining blends. The extreme temperature sensitivity of phenolic profiles (p = 0.0014) without corresponding yield changes suggests MF-derived phenolics were particularly susceptible to thermal degradation, potentially forming non-phenolic secondary products at higher temperatures. These findings collectively demonstrate that EFB-MF blends require distinct optimization strategies focused primarily on preserving target compounds rather than maximizing yield, with 300 °C being clearly preferable for phenolic retention despite its yield parity with 400 °C.

3.10. Possible Chemical Mechanisms of Oil Palm Solid Waste Decomposition into Liquid Smoke

Principal component analysis (PCA) was applied to the GC-MS dataset to clarify the relationships among the EFB-to-KS ratios, EFB-to-MF ratios, and MAP temperatures (treated as samples), alongside the normalised mass percentages of chemical compounds in the liquid smoke (treated as variables), through dimensionality reduction. The analysis reduced the dataset to thirteen principal

components. The first principal component (PC1) accounted for the largest proportion of variance, explaining 54.55% of the total variability. The second component (PC2), orthogonal to PC1, explained a further 35.06% of the variance. Figures 12, 13, and 14 present the PCA results, including the score plot, loading plot, and an enlarged view of the loading plot for PC1 and PC2. The score plot illustrates the distribution of the samples, where greater separation indicates more pronounced differences in the normalised concentrations of the identified compounds. The loading plots, both standard and magnified, highlight the extent to which each chemical compound contributes to the observed variance. Compounds located further from the origin exert a stronger influence on PC1 and PC2, with their correlation (positive or negative) interpreted based on their position relative to the sample distribution in the score plot.

As shown in Figure 12, the samples are generally widely dispersed along the PC1 and PC2 axes, indicating that each combination of treatment parameters (EFB-to-KS ratios, EFB-to-MF ratios, and MAP temperatures) yielded liquid smoke with distinct chemical compositions. Several directional arrows were incorporated to trace changes in score positions resulting from decreasing EFB content in the pyrolysed solid waste mixtures. As the EFB proportion decreased in the EFB-KS mixtures

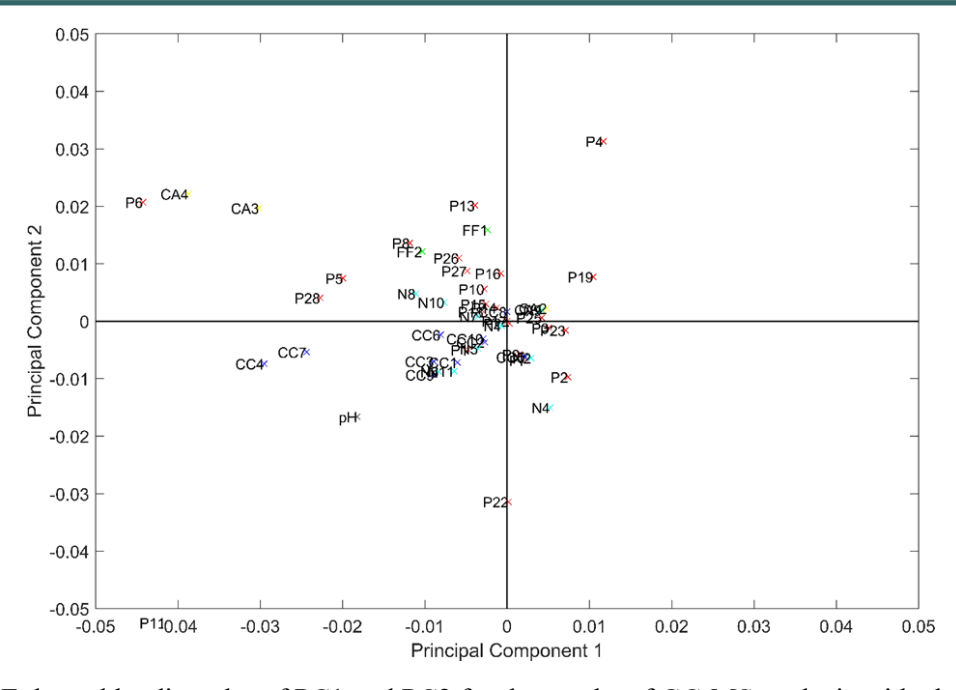
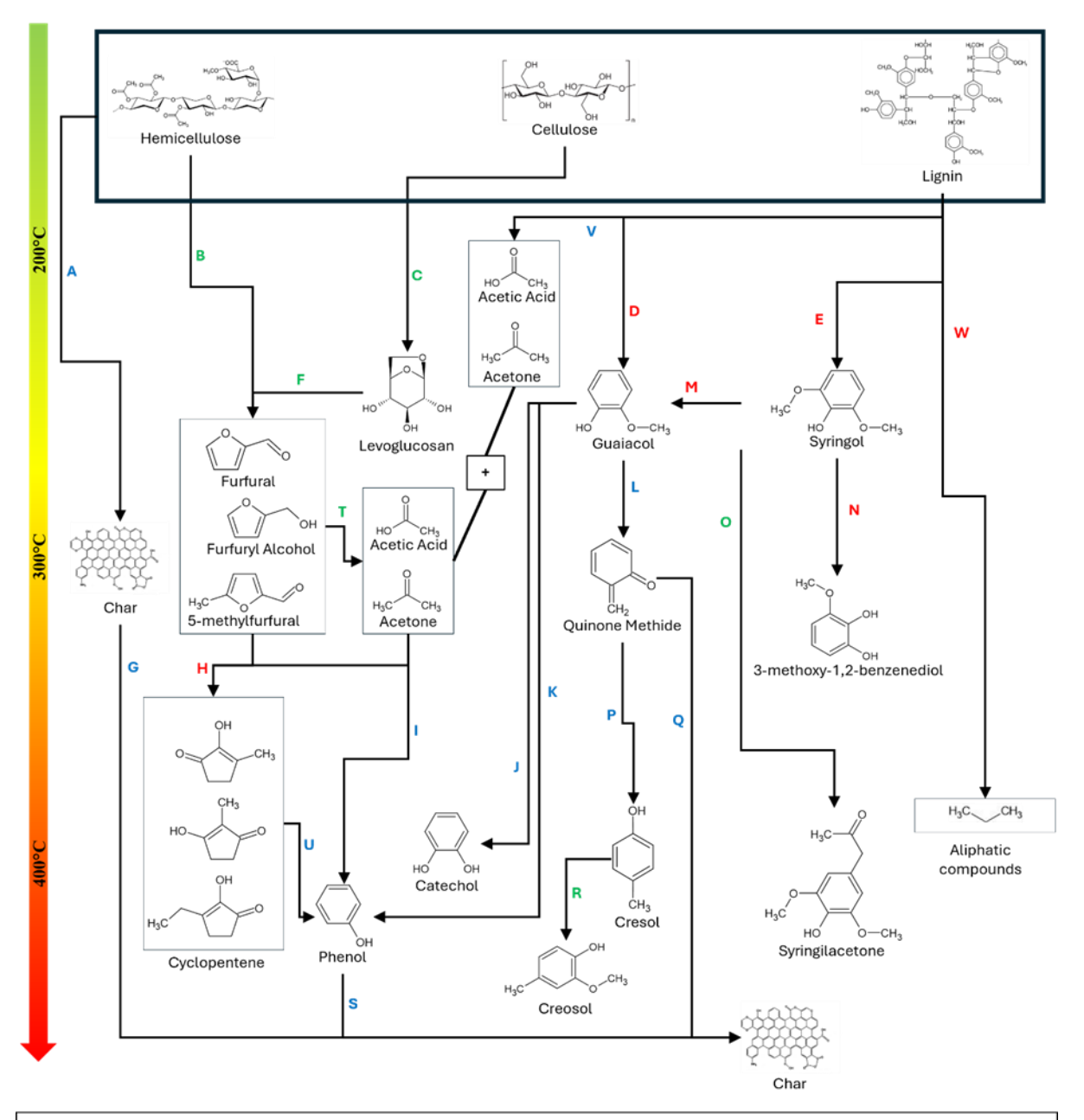


Figure 14. Enlarged loading plot of PC1 and PC2 for the results of GC-MS analysis with chemical compound IDs listed in Table 4 and 5 and the antioxidant capacity.



A: polymerization; B: depolymerization and ring opening; C: depolymerization; D: decomposition; E: decomposition; F: ring-opening; G: polymerization; H: aldol condensation, cyclization, and dehydration; I: aromatization; J,K: demethylation; L: dehydrogenation; M: demethoxylation; N: demethylation; C: demethylation; P: proton addition; Q: polymerization; R: methoxylation; S: polymerization; T: ring-opening; U: aromatization; V: debranching; W: side-chain removal; RED: in which the product is favored due to high EFB content; BLUE: in which the product is favored due to high MF content; GREEN: in which the product is favored due to high MF content

Figure 15. The possible mechanism of thermal degradation of mixtures of EFBs and either KSs or MFs during MAP.

subjected to MAP at 300 °C, the corresponding scores progressively shifted northward and eastward, following route A in the eastern quadrants. This trend suggests that the presence of EFBs was a major contributor to the score variability explained by PC2. At 400 °C, the scores associated with the same mixtures shifted in a northeasterly direction along route B, indicating that the elevated temperature enhanced the

variability explained by PC1—possibly due to increased conversion of solid waste, resulting in the formation of more chemical compounds associated with PC1. For the EFB–MF mixtures at 300 °C, the score shifts followed route C, moving in a north-westerly direction as EFB content decreased, before turning eastward for the pure MF sample. This behaviour reflects score variability primarily influenced by PC1. When pyrolysed at 400 °C, the



EFB–MF mixtures exhibited relatively minor score shifts within the western quadrants, denoted by route D. The irregular pattern of this movement may suggest limited variability explained by both PC1 and PC2.

As illustrated in Figure 13, the mass percentages of most chemical compounds are concentrated near the origin, reflecting limited variability within the dataset and a relatively minor influence on PC1 and PC2. However, certain variables—including the mass percentage of phenol (P20), the proportion of impurities, and the AC—are located at greater distances from the origin, indicating a more pronounced impact on the variance explained by PC1 and PC2. Notably, P20 exhibits a strong positive correlation with PC1, as evidenced by its prominent position in the eastern quadrant. According to Table 4 and 5, decreases in P20 content led to a spatial shift in sample distribution, from those with KS appearing in the eastern quadrants to those with MF in the western quadrants in Figure 12. In contrast, the positioning of impurities far into the western quadrant of Figure 13 reflects a notable negative correlation with PC1. The association between P20 and impurity content may point to the aromatisation of aliphatic compounds—likely the impurities—occurring through hydrogen transfer from the phenylpropane side chain during the breakdown of cellulose monomers [97]. The proximity of the EFB,400 and EFB50MF50,400 scores to the loading of impurity mass percentage suggests that both EFB and MF could contribute to impurity generation, potentially to their rich cellulose composition. Furthermore, the placement of the AC score in the quadrants highlights the importance of KS and MF in enhancing the antioxidant capacity of the liquid smoke.

Figure 14 offers a magnified representation of Figure 13, providing a clearer view of the mass percentage distribution of chemical compounds near the centre of the loading plot. These patterns are examined alongside findings from prior studies [82][98]-[101] to suggest a plausible degradation pathway triggered by MAP of mixtures containing EFBs with either KSs or MFs. According to Figure 14. most phenolic compounds, particularly prominent lignin derivatives such as methylphenol 2,6-dimethylphenol, and appear across all quadrants, in contrast to cyclopentene, which are distinctly grouped in the southeast quadrant. This contrast may indicate that phenolic compounds and cyclopentene follow opposing formation routes. Additionally, carboxylic acids like *n*-hexadecanoic acid and octadecanoic acid are in the northwest quadrant, whereas methyl esters cluster in the northeast. This spatial separation suggests that esterification of these acids is more prevalent in biomass with a high MF content.

Figure 15 provides a schematic representation of the degradation pathways of the key components in EFBs, KSs, and MFs, specifically cellulose, hemicellulose, and lignin. These pathways are derived from the compound distributions illustrated in Figures 13 and 14 and are consistent with the trends outlined in Figure 12. MAP temperatures are inversely related to PC1, whereas EFB content negatively correlates with PC2. As the MAP temperature approaches 300 °C, cellulose and hemicellulose degrade into smaller C5 and C6 sugar units such as xylose and levoglucosan, primarily through dehydration and cleavage of glycosidic bonds. These sugars then undergo ring-opening reactions, forming furfural compounds that are subsequently converted into ketones and aldehydes. Around 400 °C, these intermediates, e.g., furfural compounds, ketones, and aldehydes, are likely transformed into cyclopentene, particularly in samples rich in EFB. Moreover, ketones and aldehydes may also yield phenols and other related aromatic compounds. The pronounced phenol content in the resulting liquid smoke suggests that these pathways favour phenol production. The decomposition of lignin is significantly affected by temperature and by the relative proportions of its structural subunits: guaiacyl (G), syringyl (S), and p -hydroxyphenyl (H). Between 200 and 300 °C, lignin undergoes ether bond cleavage, generating 2methoxyphenol (guaiacol) and 2,6dimethoxyphenol (syringol). This is in line with the lignin profile of EFB, which is primarily composed of guaiacyl and syringyl units with a G-to-S ratio of 0.411 ± 0.003 [102]. Although syringol are theoretically expected to be present in nearly double the mass fraction of guaiacol in the liquid smoke, the actual dominance of guaiacol suggests that syringol may be undergoing conversion into guaiacol [100]. At approximately 300 °C, guaiacol

can be further transformed into phenol, catechol, and cresol which are more typically associated with pyrolysis temperatures above 400 °C. The elevated phenol content and relatively low levels of catechol and cresol in liquid smoke derived from samples with low EFB-to-KS ratios indicate a preference for phenol formation, likely due to demethoxylation molecular rearrangement guaiacol. of Conversely, in similarly composed samples with high antioxidant activity, higher concentrations of catechol and cresol suggest improved selectivity for these compounds during guaiacol transformation. Catechol is probably formed through demethylation of guaiacol, whereas cresol is likely produced via a radical pathway involving guaiacol conversion to quinone methide followed by hydrogenation. The cresol may then be methoxylated into creosol, a reaction favoured when the EFB-to-MF ratio is low. Within the temperature range of 300 to 400 °C, 2,6dimethoxyphenol may also undergo conversion into 3-methoxy-1,2-benzenediol and syringylacetone through demethoxylation and the addition of carbonyl side chains.

3.11. Preliminary Economic Insight

The economic viability of MAP for liquid smoke production from oil palm solid waste (EFBs, KSs, and MFs) presents both opportunities challenges that warrant careful consideration. From feedstock perspective, these agricultural byproducts are abundantly available in palm oilproducing regions at minimal or even negative cost, as mills typically incur expenses for their disposal [103]. Utilising these wastes could reduce raw material costs compared to purpose-grown biomass feedstocks. However, collection, transportation, and preprocessing costs must be factored into the overall economic equation, particularly for decentralized production scenarios. The high moisture content of fresh oil palm solid waste, particularly EFBs, may necessitate additional drying steps, potentially impacting energy budgets [104]. The energy efficiency of MAP offers significant advantages over conventional pyrolysis methods. Microwave-specific energy consumption for biomass pyrolysis typically ranges between 1.5-3.0 kWh/kg, with around 90% energy savings compared to electrical heating methods due to selective and volumetric heating characteristics

[105]. However, the capital costs for industrial-scale microwave systems remain higher than conventional reactors, with payback periods highly dependent on operational scale and product value [106]. Process optimization studies suggest that careful tuning of microwave power and residence time can significantly improve both energy efficiency and product yields [107]. The potential integration with existing palm oil mill operations could further enhance economic viability by utilizing waste heat and shared infrastructure.

Market prospects for palm-derived liquid smoke appear promising but require careful product positioning. According to Global Info Research, the global liquid smoke market, valued approximately \$80 million in 2023, is projected to grow at 6-8% annually, driven by increasing demand for natural food preservatives. Palm-based products could capture niche markets in tropical regions where wood-derived liquid smoke imports are expensive. However, product differentiation will be crucial, with our study demonstrating that EFB-KS blends can produce liquid smoke with antioxidant capacities (up to 55.92%) competitive with premium wood-derived products [108]. Potential applications extend beyond preservation to include agricultural uses as biopesticides and animal feed additives, potentially expanding market opportunities. Future technoeconomic analyses should incorporate detailed lifecycle assessments and market studies to fully evaluate commercial potential, particularly comparison to established wood-derived liquid smoke production systems.

4. CONCLUSIONS

This study demonstrated that MAP of oil palm solid waste, specifically mixtures of EFBs with KSs, or MFs, can effectively produce liquid smoke with distinct chemical and functional properties. The results showed that MAP temperature plays a critical role in determining liquid smoke yield and compound selectivity. Higher temperatures (400 °C) generally increased liquid smoke yields due to more complete thermal degradation of biomass, though excessive heating could also promote the formation of non-condensable gases and impurities. The blending ratio of raw materials significantly



influenced the chemical composition of the liquid smoke. KS-rich mixtures consistently produced higher concentrations of phenolic compounds, particularly phenol, catechol, and cresol, due to their lignin-rich structure. The MF-rich mixtures yielded more diverse compounds, including cyclopentenones and carboxylic acids, while EFBrich mixtures tended to produce more carbonylcontaining compounds and impurities, reflecting their higher holocellulose content. Antioxidant capacity of the liquid smoke was closely tied to both temperature and feedstock composition. KS and MF contributed to higher antioxidant activity, especially at moderate temperatures, due to the presence of ortho-dihydroxy and methoxysubstituted phenolics. In contrast, EFB-rich mixtures showed lower antioxidant performance, particularly at elevated temperatures, thermolabile compounds were more prone to degradation. Overall, MAP enables conversion of oil palm solid waste into functional liquid smoke, with temperature and feedstock blending ratio serving as key levers to tune product yield and quality. Based on the compounds identified in the liquid smoke, the study proposed a thermal degradation mechanism for MAP of oil palm solid waste. This mechanism includes detailed insights into how MAP temperature and blending ratios (EFB-to-KS and EFB-to-MF) influence specific chemical conversion pathways. These findings offer valuable insights for optimisation of MAP processes and feedstock formulations to enhance the utility of liquid smoke in food, agricultural, and industrial applications.

AUTHOR INFORMATION

Corresponding Author

Orchidea Rachmaniah — Department of Chemical Engineering, Institut Teknologi Sepuluh Nopember, Surabaya-60111 (Indonesia);

orcid.org/0000-0002-3849-8970 Email: orchidea@its.ac.id

Authors

Wahyu Meka — Department of Chemical Engineering, Institut Teknologi Sepuluh Nopember, Surabaya-60111 (Indonesia);

orcid.org/0000-0001-6195-9715

Berlian Widi Bela Pamungkas — Department of Chemical Engineering, Institut Teknologi Sepuluh Nopember, Surabaya-60111 (Indonesia);

orcid.org/0009-0007-7126-2031

Faisal Akbar — Department of Chemical Engineering, Institut Teknologi Sepuluh Nopember, Surabaya-60111 (Indonesia);

orcid.org/0009-0005-7258-7511

Adidoyo Prakoso — Department of Chemical Engineering, Institut Teknologi Sepuluh Nopember, Surabaya-60111 (Indonesia);

orcid.org/0009-0008-1478-0788

Latifa Hanum Lalasari — Research Center for Metallurgy, National Research and Innovation Agency, Tangerang Selatan-15314 (Indonesia);

orcid.org/0000-0002-0648-8655

Sri Fitria Retnawaty — Faculty of Mathematics, Natural Science, and Health, Universitas Muhammadiyah Riau, Pekanbaru-28290 (Indonesia);

orcid.org/0000-0001-7464-2127

Shanti Faridah binti Salleh — Department of Chemical Engineering and Energy Sustainability, University Malaysia Sarawak, Kota Samarahan-94300 (Malaysia);

orcid.org/0000-0002-6003-2464

Salman Masoudi Soltani — Department of Chemical Engineering, Brunel University of London, London-UB8 3PH (United Kingdom);

orcid.org/0000-0002-5983-0397

Paul Fennell — Department of Chemical Engineering, Imperial College London, London-SW7 2AZ (United Kingdom);

© orcid.org/0000-0002-6001-5285

Author Contributions

W. Conceptualization, M. and O. R.; M.; Methodology, W. Formal Analysis, Investigation, and Data Curation, B. W. B. P., F. A., and A. P.; Resources, L. H. L.; Writing - Original Draft Preparation, Visualization, and Funding Acquisition, W. M.; Writing – Review & Editing, S. F. R., S. F. binti S., S. M. S., and P. F.; Supervision, and Project Administration, W. M. and O.R.

Conflicts of Interest

The authors declare no conflict of interest.

ACKNOWLEDGEMENT

The authors would like to express their gratitude to Institut Teknologi Sepuluh Nopember for fully funding the research associated with this paper via the scheme of Dana Keilmuan ITS (1688/PKS/ITS/2023) organised by Direktorat Riset dan Pengabdian kepada Masyarakat.

REFERENCES

- [1] J. Trávníček, B. Schlatter, M. Helbing, and H. Willer. (2025). In: "The World of Organic Agriculture. Statistics and Emerging Trends 2025". Research Institute of Organic Agriculture FiBL and IFOAM Organics International.
- [2] J. Kearney. (2010). "Food consumption trends and drivers". *Philosophical Transactions of the Royal Society B: Biological Sciences.* **365** (1554): 2793-807. 10.1098/rstb.2010.0149.
- [3] P. Bryla. (2016). "Organic food consumption in Poland: Motives and barriers". *Appetite*. **105**: 737-46. 10.1016/j.appet.2016.07.012.
- [4] J. M. Lingbeck, P. Cordero, C. A. O'Bryan, M. G. Johnson, S. C. Ricke, and P. G. Crandall. (2014). "Functionality of liquid smoke as an all-natural antimicrobial in food preservation". *Meat Science.* **97** (2): 197-206. 10.1016/j.meatsci.2014.02.003.
- [5] K. Tiilikkala, L. Fagernäs, and J. Tiilikkala. (2010). "History and Use of Wood Pyrolysis Liquids as Biocide and Plant Protection Product". *The Open Agriculture Journal.* 4 (1): 111-118. 10.2174/1874331501004010111.
- [6] G. V. Research. (2019). "Liquid Smoke Market Size, Share & Trends Analysis Report by Application (Meat Products, Sauces, Dairy Products, Pet Food), By Region, And Segment Forecasts, 2019 -2025". Grand View Research.
- [7] A. S. Pimenta, T. V. d. C. Monteiro, M. Fasciotti, R. M. Braga, E. C. d. Souza, and K. M. G. d. Lima. (2018). "Fast pyrolysis of

- trunk wood and stump wood from a Brazilian eucalyptus clone". *Industrial Crops and Products.* **125** : 630-638. <u>10.1016/</u> j.indcrop.2018.08.083.
- [8] S. Czernik and A. V. Bridgwater. (2004). "Overview of Applications of Biomass Fast Pyrolysis Oil". *Energy & Fuels.* 18 (2): 590-598. 10.1021/ef034067u.
- [9] X. Xin, K. Dell, I. A. Udugama, B. R. Young, and S. Baroutian. (2021). "Transforming biomass pyrolysis technologies to produce liquid smoke food flavouring". *Journal of Cleaner Production*. **294**. 10.1016/j.jclepro.2020.125368.
- [10] J. G. Canadell and M. R. Raupach. (2008). "Managing forests for climate change mitigation". *Science*. 320 (5882): 1456-7. 10.1126/science.1155458.
- [11] F. Hua, L. A. Bruijnzeel, P. Meli, P. A. Martin, J. Zhang, S. Nakagawa, X. Miao, W. Wang, C. McEvoy, J. L. Pena-Arancibia, P. H. S. Brancalion, P. Smith, D. P. Edwards, and A. Balmford. (2022). "The biodiversity and ecosystem service contributions and trade-offs of forest restoration approaches". *Science*. 376 (6595): 839-844. 10.1126/science.abl4649.
- [12] R. Nabila, W. Hidayat, A. Haryanto, U. Hasanudin, D. A. Iryani, S. Lee, S. Kim, S. Kim, D. Chun, H. Choi, H. Im, J. Lim, K. Kim, D. Jun, J. Moon, and J. Yoo. (2023). "Oil palm biomass Indonesia: Thermochemical upgrading and its utilization". Renewable and Sustainable Energy Reviews. 176. 10.1016/ j.rser.2023.113193.
- [13] E. Hambali and M. Rivai. (2017). "The Potential of Palm Oil Waste Biomass in Indonesia in 2020 and 2030". IOP Conference Series: Earth and Environmental Science. 65. 10.1088/1755-1315/65/1/012050.
- [14] J. A. Garcia-Nunez, M. R. Pelaez-Samaniego, M. E. Garcia-Perez, I. Fonts, J. Abrego, R. J. M. Westerhof, and M. Garcia-Perez. (2017). "Historical Developments of Pyrolysis Reactors: A Review". *Energy & Fuels.* 31 (6): 5751-5775. 10.1021/acs.energyfuels.7b00641.



- [15] J. P. Cao, X. B. Xiao, S. Y. Zhang, X. Y. Zhao, K. Sato, Y. Ogawa, X. Y. Wei, and T. Takarada. (2011). "Preparation and characterization of bio-oils from internally circulating fluidized-bed pyrolyses of municipal, livestock, and wood waste". *Bioresource Technology.* **102** (2): 2009-15. 10.1016/j.biortech.2010.09.057.
- A. M. Eaton, L. D. Smoot, S. C. Hill, and C. Eatough. (1999)."Components, formulations, solutions, evaluation, application of comprehensive combustion models". **Progress** inEnergy and 25 387-436. Combustion Science. (4): 10.1016/s0360-1285(99)00008-8.
- [17] K. E. Haque. (1999). "Microwave energy for mineral treatment processes—a brief review". *International Journal of Mineral Processing.* 57 (1): 1-24. 10.1016/s0301-7516(99)00009-5.
- [18] N. Bengtsson. (2001). "Development of industrial microwave heating of foods in Europe over the past 30 years". *Journal of Microwave Power and Electromagnetic Energy*. 36 (4): 227-40. 10.1080/08327823.2001.11688464.
- [19] D. R. Nhuchhen, M. T. Afzal, T. Dreise, and A. A. Salema. (2018). "Characteristics of biochar and bio-oil produced from wood pellets pyrolysis using a bench scale fixed bed, microwave reactor". *Biomass and Bioenergy.* 119 : 293-303. 10.1016/j.biombioe.2018.09.035.
- [20] Z. Yang, H. Lei, Y. Zhang, K. Qian, E. Villota, M. Qian, G. Yadavalli, and H. Sun. (2018). "Production of renewable alkylphenols from catalytic pyrolysis of Douglas fir sawdust over biomass-derived activated carbons". *Applied Energy.* **220**: 426-436. 10.1016/j.apenergy.2018.03.107.
- [21] A. Al Shra'ah and R. Helleur. (2014). "Microwave pyrolysis of cellulose at low temperature". *Journal of Analytical and Applied Pyrolysis.* **105**: 91-99. <u>10.1016/j.jaap.2013.10.007</u>.
- [22] F. P. Bouxin, J. H. Clark, J. Fan, and V. Budarin. (2019). "Combining steam distillation with microwave-assisted pyrolysis to maximise direct production of

- levoglucosenone from agricultural wastes". *Green Chemistry*. **21** (6): 1282-1291. 10.1039/c8gc02994f.
- [23] M. De bruyn, J. Fan, V. L. Budarin, D. J. Macquarrie, L. D. Gomez, R. Simister, T. J. Farmer, W. D. Raverty, S. J. McQueen-Mason, and J. H. Clark. (2016). "A new perspective in bio-refining: levoglucosenone and cleaner lignin from waste biorefinery hydrolysis lignin by selective conversion of residual saccharides". *Energy & Environmental Science*. 9 (8): 2571-2574. 10.1039/c6ee01352j.
- [24] S. Gadkari, B. Fidalgo, and S. Gu. (2017). "Numerical investigation of microwave-assisted pyrolysis of lignin". *Fuel Processing Technology.* **156** : 473-484. <u>10.1016/j.fuproc.2016.10.012</u>.
- [25] V. L. Budarin, J. H. Clark, B. A. Lanigan, P. Shuttleworth, and D. J. Macquarrie. (2010). "Microwave assisted decomposition of cellulose: A new thermochemical route for biomass exploitation". *Bioresource Technology.* **101** (10): 3776-9. <u>10.1016/j.biortech.2009.12.110</u>.
- [26] Q. Bu, H. Lei, L. Wang, Y. Wei, L. Zhu, X. Zhang, Y. Liu, G. Yadavalli, and J. Tang. (2014). "Bio-based phenols and fuel production from catalytic microwave pyrolysis of lignin by activated carbons". *Bioresource Technology.* **162**: 142-7. 10.1016/j.biortech.2014.03.103.
- [27] F. Delbecq and C. Len. (2018). "Recent Advances in the Microwave-Assisted Production of Hydroxymethylfurfural by Hydrolysis of Cellulose Derivatives-A Review". *Molecules*. **23** (8). 10.3390/molecules23081973.
- [28] W. Yunpu, D. A. I. Leilei, F. A. N. Liangliang, S. Shaoqi, L. I. U. Yuhuan, and R. Roger. (2016). "Review of microwave-assisted lignin conversion for renewable fuels and chemicals". *Journal of Analytical and Applied Pyrolysis.* 119: 104-113. 10.1016/j.jaap.2016.03.011.
- [29] E. R. Sari. (2018). "Identifikasi Kualitas Biobriket Hasil Pirolisis Limbah Tandan Kosong Kelapa Sawit Dengan Variasi Dimensi". *AGRITEPA: Jurnal Ilmu dan*

- *Teknologi Pertanian.* **4** (1): 146-157. 10.37676/agritepa.v4i1.594.
- [30] L. Ni'mah, M. F. Setiawan, and S. P. Prabowo. (2019). "Utilization of Waste Palm Kernel Shells and Empty Palm Oil Bunches as Raw Material Production of Liquid Smoke". *IOP Conference Series: Earth and Environmental Science*. **366**. 10.1088/1755-1315/366/1/012032.
- [31] M. Faisal, A. Gani, F. Mulana, H. Desvita, and S. Kamaruzzaman. (2020). "Effects of Pyrolysis Temperature on the Composition of Liquid Smoke Derived from Oil Palm Empty Fruit Bunches". *Rasayan Journal of chemistry.* **13** (01): 514-520. 10.31788/rjc.2020.1315507.
- [32] S. Maulina and E. R. Kamny. (2020). "Quality improvement of smoke liquid from oil palm fronds pyrolysis through adsorption distillation process by using zeolite as adsorbent". *IOP Conference Series: Materials Science and Engineering.* **801**. 10.1088/1757-899x/801/1/012063.
- [33] Z. A. N. M. Majid, L. Rahmawati, and C. Riyani. (2022). "Identification of bio-oil chemical compounds from pyrolysis process of oil palm empty fruit bunches". *IOP Conference Series: Earth and Environmental Science*. **1063** (1). 10.1088/1755-1315/1063/1/012001.
- [34] A. T. Hoang, H. C. Ong, I. M. R. Fattah, C. T. Chong, C. K. Cheng, R. Sakthivel, and Y. S. Ok. (2021). "Progress on the lignocellulosic biomass pyrolysis for biofuel production toward environmental sustainability". Fuel Processing Technology. 223. 10.1016/j.fuproc.2021.106997.
- [35] X. Xin, A. Bissett, J. Wang, A. Gan, K. Dell, and S. Baroutian. (2021). "Production of liquid smoke using fluidised-bed fast pyrolysis and its application to green lipped mussel meat". *Food Control.* **124**. <u>10.1016/j.foodcont.2021.107874</u>.
- [36] A. V. Bridgwater. (2012). "Review of fast pyrolysis of biomass and product upgrading". *Biomass and Bioenergy*. **38**: 68-94. 10.1016/j.biombioe.2011.01.048.
- [37] N. Montazeri, A. C. Oliveira, B. H. Himelbloom, M. B. Leigh, and C. A. Crapo.

- (2013). "Chemical characterization of commercial liquid smoke products". *Food Science & Nutrition*. **1** (1): 102-15. <u>10.1002/</u>fsn3.9.
- [38] F. Xiao, T. Xu, B. Lu, and R. Liu. (2020). "Guidelines for antioxidant assays for food components". *Food Frontiers*. **1** (1): 60-69. 10.1002/fft2.10.
- [39] Y.-M. Kim, T. U. Han, B. Hwang, B. Lee, H. W. Lee, Y.-K. Park, and S. Kim. (2016). "Pyrolysis kinetics and product properties of softwoods, hardwoods, and the nut shell of softwood". *Korean Journal of Chemical Engineering*. **33** (8): 2350-2358. 10.1007/s11814-016-0142-2.
- [40] L. P. Santi, D. N. Kalbuadi, and D. H. Goenadi. (2019). "Empty Fruit Bunches as Potential Source for Biosilica Fertilizer for Oil Palm". *Journal of Tropical Biodiversity and Biotechnology*. **4** (3). 10.22146/jtbb.38749.
- [41] D. A. C. Manning. (2010). "Mineral sources of potassium for plant nutrition. A review". *Agronomy for Sustainable Development.* **30** (2): 281-294. 10.1051/agro/2009023.
- [42] S. Patnaik, S. Kumar, and A. K. Panda. (2020). "Thermal degradation of eco-friendly alternative plastics: kinetics and thermodynamics analysis". *Environmental Science and Pollution Research.* 27 (13): 14991-15000. 10.1007/s11356-020-07919-w.
- [43] D. Vamvuka, E. Kakaras, E. Kastanaki, and P. Grammelis. (2003). "Pyrolysis characteristics and kinetics of biomass residuals mixtures with lignite □". Fuel. 82 (15-17): 1949-1960. 10.1016/s0016-2361(03) 00153-4.
- [44] F. Surahmanto, H. Saptoadi, H. Sulistyo, and T. A. Rohmat. (2017). "Investigation of the slow pyrolysis kinetics of oil palm solid waste by the distributed activation energy model". *Biofuels*. **11** (6): 663-670. 10.1080/17597269.2017.1387750.
- [45] A. A. Salema and F. N. Ani. (2012). "Pyrolysis of oil palm empty fruit bunch biomass pellets using multimode microwave irradiation". *Bioresource Technology.* **125**: 102-7. 10.1016/j.biortech.2012.08.002.



- [46] J. Akhtar and N. Saidina Amin. (2012). "A review on operating parameters for optimum liquid oil yield in biomass pyrolysis". *Renewable and Sustainable Energy Reviews.*16 (7): 5101-5109. 10.1016/j.rser.2012.05.033.
- [47] W. A. Khanday, G. Kabir, and B. H. Hameed. (2016). "Catalytic pyrolysis of oil palm mesocarp fibre on a zeolite derived from low-cost oil palm ash". *Energy Conversion and Management.* **127**: 265-272. 10.1016/j.enconman.2016.08.093.
- [48] G. Kabir, A. T. Mohd Din, and B. H. Hameed. (2017). "Pyrolysis of oil palm mesocarp fiber and palm frond in a slow-heating fixed-bed reactor: A comparative study". *Bioresource Technology.* **241**: 563-572. 10.1016/j.biortech.2017.05.180.
- [49] H. Yang, R. Yan, H. Chen, D. H. Lee, and C. Zheng. (2007). "Characteristics of hemicellulose, cellulose and lignin pyrolysis". Fuel. 86 (12-13): 1781-1788. 10.1016/j.fuel.2006.12.013.
- [50] J. D. Coral Medina, A. L. Woiciechowski, A. Zandona Filho, L. Bissoqui, M. D. Noseda, L. P. de Souza Vandenberghe, S. F. Zawadzki, and C. R. Soccol. (2016). "Biological activities and thermal behavior of lignin from oil palm empty fruit bunches as potential source of chemicals of added value". *Industrial Crops and Products.* 94: 630-637. 10.1016/j.indcrop.2016.09.046.
- [51] K. Wu, K. Yang, Y. Zhu, B. Luo, C. Chu, M. Li, Y. Zhang, and H. Zhang. (2023). "The copyrolysis interactions of isolated lignins and cellulose by experiments and theoretical calculations". *Energy.* 263. <u>10.1016/j.energy.2022.125811.</u>
- [52] B. Babinszki, E. Jakab, V. Terjék, Z. Sebestyén, G. Várhegyi, Z. May, A. Mahakhant, L. Attanatho, A. Suemanotham, Y. Thanmongkhon, and Z. Czégény. (2021). "Thermal decomposition of biomass wastes derived from palm oil production". *Journal of Analytical and Applied Pyrolysis.* 155. 10.1016/j.jaap.2021.105069.
- [53] J. Alvarez, M. Amutio, G. Lopez, L. Santamaria, J. Bilbao, and M. Olazar. (2019). "Improving bio-oil properties through the fast

- co-pyrolysis of lignocellulosic biomass and waste tyres". *Waste Management.* **85**: 385-395. 10.1016/j.wasman.2019.01.003.
- [54] I. de Menezes Nogueira, F. Avelino, D. R. de Oliveira, N. F. Souza, M. F. Rosa, S. E. Mazzetto, and D. Lomonaco. (2019). "Organic solvent fractionation of acetosolv palm oil lignin: The role of its structure on the antioxidant activity". *International Journal of Biological Macromolecules.* 122: 1163-1172. 10.1016/j.ijbiomac.2018.09.066.
- [55] H. L. Trajano, N. L. Engle, M. Foston, A. J. Ragauskas, T. J. Tschaplinski, and C. E. Wyman. (2013). "The fate of lignin during hydrothermal pretreatment". *Biotechnology for Biofuels*. 6 (1): 110. 10.1186/1754-6834-6-110.
- [56] J. S. L. Chang, Y. S. Chan, M. C. Law, and C. P. Leo. (2017). "Comparative microstructure study of oil palm fruit bunch fibre, mesocarp and kernels after microwave pre-treatment". *IOP Conference Series: Materials Science and Engineering.* 217. 10.1088/1757-899x/217/1/012026.
- [57] N. A. F. Abdul Samad and S. Saleh. (2022). "Analysis of volatile composition released from torrefaction of empty fruit bunch". *Materials Today: Proceedings.* 57: 1202-1207. 10.1016/j.matpr.2021.10.462.
- [58] A. Demirbas. (2007). "The influence of temperature on the yields of compounds existing in bio-oils obtained from biomass samples via pyrolysis". *Fuel Processing Technology.* **88** (6): 591-597. 10.1016/j.fuproc.2007.01.010.
- [59] S. Konsomboon, S. Pipatmanomai, T. Madhiyanon, and S. Tia. (2011). "Effect of kaolin addition on ash characteristics of palm empty fruit bunch (EFB) upon combustion". Applied Energy. 88 (1): 298-305. 10.1016/j.apenergy.2010.07.008.
- [60] R. J. Evans and T. A. Milne. (2002). "Molecular characterization of the pyrolysis of biomass". *Energy & Fuels.* 1 (2): 123-137. 10.1021/ef00002a001.
- [61] Z. Gao, N. Li, S. Yin, and W. Yi. (2019). "Pyrolysis behavior of cellulose in a fixed bed reactor: Residue evolution and effects of parameters on products distribution and bio-

- oil composition". *Energy*. **175** : 1067-1074. 10.1016/j.energy.2019.03.094.
- [62] R. S. Assary and L. A. Curtiss. (2011). "Thermochemistry and Reaction Barriers for the Formation of Levoglucosenone from Cellobiose". *ChemCatChem.* 4 (2): 200-205. 10.1002/cctc.201100280.
- [63] H. B. Mayes, M. W. Nolte, G. T. Beckham, B. H. Shanks, and L. J. Broadbelt. (2014).
 "The Alpha–Bet(a) of Glucose Pyrolysis: Computational and Experimental Investigations of 5-Hydroxymethylfurfural and Levoglucosan Formation Reveal Implications for Cellulose Pyrolysis". ACS Sustainable Chemistry & Engineering. 2 (6): 1461-1473. 10.1021/sc500113m.
- [64] Q. Lu, H.-t. Liao, Y. Zhang, J.-j. Zhang, and C.-q. Dong. (2013). "Reaction mechanism of low-temperature fast pyrolysis of fructose to produce 5-hydroxymethyl furfural". *Journal* of Fuel Chemistry and Technology. 41 (9): 1070-1076. 10.1016/s1872-5813(13)60044-4.
- [65] B. Hu, Q. Lu, X. Jiang, X. Dong, M. Cui, C. Dong, and Y. Yang. (2018). "Pyrolysis mechanism of glucose and mannose: The formation of 5-hydroxymethyl furfural and furfural". *Journal of Energy Chemistry.* 27 (2): 486-501. 10.1016/j.jechem.2017.11.013.
- [66] D. K. Shen and S. Gu. (2009). "The mechanism for thermal decomposition of cellulose and its main products". *Bioresource Technology*. **100** (24): 6496-504. <u>10.1016/j.biortech.2009.06.095</u>.
- [67] Y. Zhang, C. Liu, and H. Xie. (2014). "Mechanism studies on β-d-glucopyranose pyrolysis by density functional theory methods". *Journal of Analytical and Applied Pyrolysis*. **105** : 23-34. <u>10.1016/j.jaap.2013.09.016</u>.
- [68] I. Polaert, L. Estel, R. Huyghe, and M. Thomas. (2010). "Adsorbents regeneration under microwave irradiation for dehydration and volatile organic compounds gas treatment". *Chemical Engineering Journal*. 162 (3): 941-948. 10.1016/j.cej.2010.06.047.
- [69] D. K. Shen, S. Gu, and A. V. Bridgwater. (2010). "Study on the pyrolytic behaviour of xylan-based hemicellulose using TG-FTIR and Py-GC-FTIR". *Journal of Analytical*

- *and Applied Pyrolysis.* **87** (2): 199-206. 10.1016/j.jaap.2009.12.001.
- [70] J. Y. Yeo, B. L. F. Chin, J. K. Tan, and Y. S. Loh. (2019). "Comparative studies on the pyrolysis of cellulose, hemicellulose, and lignin based on combined kinetics". *Journal of the Energy Institute.* **92** (1): 27-37. 10.1016/j.joei.2017.12.003.
- [71] M. De Bruyn, V. L. Budarin, G. S. J. Sturm, G. D. Stefanidis, M. Radoiu, A. Stankiewicz, and D. J. Macquarrie. (2017). "Subtle Microwave-Induced Overheating Effects in an Industrial Demethylation Reaction and Their Direct Use in the Development of an Innovative Microwave Reactor". *Journal of the American Chemical Society.* 139 (15): 5431-5436. 10.1021/jacs.7b00689.
- [72] M. R. Crimmin. (2021). "Benzene rings broken for chemical synthesis". *Nature*. 597 (7874): 33-34. 10.1038/d41586-021-02322-y.
- [73] K. B. Ansari, J. S. Arora, J. W. Chew, P. J. Dauenhauer, and S. H. Mushrif. (2019). "Fast Pyrolysis of Cellulose, Hemicellulose, and Lignin: Effect of Operating Temperature on Bio-oil Yield and Composition and Insights into the Intrinsic Pyrolysis Chemistry". *Industrial & Engineering Chemistry Research.* 58 (35): 15838-15852. 10.1021/acs.iecr.9b00920.
- [74] L. T. Cureton, E. Napadensky, C. Annunziato, and J. J. La Scala. (2017). "The effect of furan molecular units on the glass transition and thermal degradation temperatures of polyamides". *Journal of Applied Polymer Science*. **134** (46). 10.1002/app.45514.
- [75] S. Wang, Y. Hu, B. B. Uzoejinwa, B. Cao, Z. He, Q. Wang, and S. Xu. (2017). "Pyrolysis mechanisms of typical seaweed polysaccharides". *Journal of Analytical and Applied Pyrolysis.* **124**: 373-383. <u>10.1016/j.jaap.2016.12.005</u>.
- [76] M. Kröger, F. Hartmann, and M. Klemm. (2013). "Hydrothermal Treatment of Carboxy -methyl Cellulose Salt: Formation and Decomposition of Furans, Pentenes and Benzenes". *Chemical Engineering & Technology*. 36 (2): 287-294. <u>10.1002/ceat.201200468</u>.



- [77] B. C. Hong, N. S. Dange, C. S. Hsu, and J. H. Liao. (2010). "Sequential organocatalytic Stetter and Michael-Aldol condensation reaction: asymmetric synthesis of fully substituted cyclopentenes via a [1 + 2 + 2] annulation strategy". *Organic Letters.* 12 (21): 4812-5. 10.1021/ol101969t.
- [78] D. K. Shen, S. Gu, K. H. Luo, S. R. Wang, and M. X. Fang. (2010). "The pyrolytic degradation of wood-derived lignin from pulping process". *Bioresource Technology*. **101** (15): 6136-46. 10.1016/j.biortech.2010.02.078.
- [79] K. M. Sabil, M. A. Aziz, B. Lal, and Y. Uemura. (2013). "Effects of torrefaction on the physiochemical properties of oil palm empty fruit bunches, mesocarp fiber and kernel shell". *Biomass and Bioenergy.* **56**: 351-360. 10.1016/j.biombioe.2013.05.015.
- [80] C. O. Edmund, M. S. Christopher, and D. K. Pascal. (2014). "Characterization of palm kernel shell for materials reinforcement and water treatment". *Journal of Chemical Engineering and Materials Science*. **5** (1): 1-6. 10.5897/jcems2014.0172.
- [81] K. C. Jun, A. A. Abdul Raman, and A. Buthiyappan. (2020). "Treatment of oil refinery effluent using bio-adsorbent developed from activated palm kernel shell and zeolite". *RSC Advances*. **10** (40): 24079-24094. 10.1039/d0ra03307c.
- [82] A. E. Harman-Ware, T. Morgan, M. Wilson, M. Crocker, J. Zhang, K. Liu, J. Stork, and S. Debolt. (2013). "Microalgae as a renewable fuel source: Fast pyrolysis of Scenedesmus sp". *Renewable Energy.* **60**: 625-632. 10.1016/j.renene.2013.06.016.
- [83] Z. Yao, X. Ma, and Z. Xiao. (2020). "The effect of two pretreatment levels on the pyrolysis characteristics of water hyacinth". *Renewable Energy.* **151**: 514-527. 10.1016/j.renene.2019.11.046.
- [84] H. Loei, J. Lim, M. Tan, T. K. Lim, Q. S. Lin, F. T. Chew, H. Kulaveerasingam, and M. C. Chung. (2013). "Proteomic analysis of the oil palm fruit mesocarp reveals elevated oxidative phosphorylation activity is critical for increased storage oil production". *Journal*

- *of Proteome Research.* **12** (11): 5096-109. 10.1021/pr400606h.
- [85] H. Kawamoto. (2017). "Lignin pyrolysis reactions". *Journal of Wood Science*. **63** (2): 117-132. 10.1007/s10086-016-1606-z.
- [86] H. Baseri, S. K. Hosseinihashemi, S. K. Hosseinashrafi, and J. J. Mehjabin. (2025). "Potential Antioxidants in Bio-oil Obtained by Pyrolysis of Yew (Taxus baccata L.) Tree Bark". *Drvna industrija*. **76** (2): 201-211. 10.5552/drvind.2025.0233.
- [87] I. A. Dias, R. P. Horta, M. Matos, C. V. Helm, W. L. E. Magalhães, E. A. de Lima, B. J. G. da Silva, G. I. B. de Muniz, and P. H. G. de Cademartori. (2023). "Exploring the antioxidant and antimicrobial properties of the water-soluble fraction derived from pyrolytic lignin separation in fast-pyrolysis bio-oil". *Biomass Conversion and Biorefinery.* 14 (19): 24333-24344. 10.1007/s13399-023-04561-7.
- [88] D. Yin, R. Xue, Y. Li, M. Zhu, and D. Li. (2023). "Valorization of Coptis chinensis extraction residue via slow pyrolysis for the production of bioactive wood vinegar". *Biomass Conversion and Biorefinery.* 14 (14): 16559-16574. 10.1007/s13399-023-03890-x.
- [89] R. H. Rosenwald, J. R. Hoatson, and J. A. Chenicek. (2002). "Alkyl Phenols as Antioxidants". *Industrial & Engineering Chemistry*. **42** (1): 162-165. 10.1021/ie50481a042.
- [90] J. Chen, J. Yang, L. Ma, J. Li, N. Shahzad, and C. K. Kim. (2020). "Structure-antioxidant activity relationship of methoxy, phenolic hydroxyl, and carboxylic acid groups of phenolic acids". *Scientific Reports*. **10** (1): 2611. 10.1038/s41598-020-59451-z.
- [91] A. Loo, K. Jain, and I. Darah. (2008). "Antioxidant activity of compounds isolated from the pyroligneous acid, Rhizophora apiculata". *Food Chemistry*. **107** (3): 1151-1160. 10.1016/j.foodchem.2007.09.044.
- [92] L. R. C. Barclay, C. E. Edwards, and M. R. Vinqvist. (1999). "Media Effects on Antioxidant Activities of Phenols and Catechols". *Journal of the American*

- *Chemical Society.* **121** (26): 6226-6231. 10.1021/ja990878u.
- [93] A. S. Alwehaibi, D. J. Macquarrie, and M. S. Stark. (2016). "Effect of spruce-derived phenolics extracted using microwave enhanced pyrolysis on the oxidative stability of biodiesel". *Green Chemistry.* **18** (9): 2762-2774. 10.1039/c5gc02520f.
- [94] E. B. Hassan, E. M. El-Giar, and P. Steele. (2016). "Evaluation of the antioxidant activities of different bio-oils and their phenolic distilled fractions for wood preservation". *International Biodeterioration & Biodegradation*. **110**: 121-128. 10.1016/j.ibiod.2016.03.015.
- [95] Y. Ohkatsu and F. Suzuki. (2011). "Synergism between Phenolic Antioxidants in Autoxidation". *Journal of the Japan Petroleum Institute*. **54** (1): 22-29. 10.1627/jpi.54.22.
- [96] J. Gierer and T. Reitberger. (1992). "The Reactions of Hydroxyl Radicals with Aromatic Rings in Lignins, Studied with Creosol and 4-Methylveratrol". *Holzforschung.* **46** (6): 495-504. 10.1515/hfsg.1992.46.6.495.
- [97] P. Xue, M. Liu, H. Yang, H. Zhang, Y. Chen, Q. Hu, S. Zhang, and H. Chen. (2023). "Mechanism study on pyrolysis interaction between cellulose, hemicellulose, and lignin based on photoionization time-of-flight mass spectrometer (PI-TOF-MS) analysis". *Fuel.* 338. 10.1016/j.fuel.2022.127276.
- [98] D. Chen, K. Cen, X. Zhuang, Z. Gan, J. Zhou, Y. Zhang, and H. Zhang. (2022). "Insight into biomass pyrolysis mechanism based on cellulose, hemicellulose, and lignin: Evolution of volatiles and kinetics, elucidation of reaction pathways, and characterization of gas, biochar and bio-oil". *Combustion and Flame.* 242. 10.1016/j.combustflame.2022.112142.
- [99] F.-X. Collard and J. Blin. (2014). "A review on pyrolysis of biomass constituents: Mechanisms and composition of the products obtained from the conversion of cellulose, hemicelluloses and lignin". *Renewable and Sustainable Energy Reviews.* **38**: 594-608. 10.1016/j.rser.2014.06.013.

- [100] M. Asmadi, H. Kawamoto, and S. Saka. (2011). "Thermal reactions of guaiacol and syringol as lignin model aromatic nuclei". *Journal of Analytical and Applied Pyrolysis*. 92 (1): 88-98. 10.1016/j.jaap.2011.04.011.
- [101] G. Song, D. Huang, Q. Ren, S. Hu, J. Xu, K. Xu, L. Jiang, Y. Wang, S. Su, and J. Xiang. (2024). "Inner-particle reaction mechanism of cellulose, hemicellulose and lignin during photo-thermal pyrolysis process: Evolution characteristics of free radicals". *Energy.* 297. 10.1016/j.energy.2024.131201.
- [102] N. M. Salleh, S. A. Ismail, and M. N. Ibrahim. (2015). "Radical scavenging activity of lignin extracted from oil palm empty fruit bunch and its effect on glutathione-Stransferase enzymes activity". *Asian Journal of Pharmaceutical and Clinical Research*. 8 (3): 81-7.
- [103] J. M. L. Thoe, N. Surugau, and H. L. H. Chong. (2019). "Application of oil palm empty fruit bunch as adsorbent: A review". *Transactions on Science and Technology.* **6** (1): 9-26.
- [104] R. Ahorsu, F. Medina, and M. Constantí. (2018). "Significance and Challenges of Biomass as a Suitable Feedstock for Bioenergy and Biochemical Production: A Review". *Energies*. 11 (12). 10.3390/en11123366.
- [105] J. M. Bermúdez, D. Beneroso, N. Rey-Raap, A. Arenillas, and J. A. Menéndez. (2015). "Energy consumption estimation in the scaling-up of microwave heating processes". *Chemical Engineering and Processing: Process Intensification.* 95: 1-8. 10.1016/j.cep.2015.05.001.
- [106] S. Mari Selvam, P. Balasubramanian, M. Chintala, and L. K. S. Gujjala. (2024). "Techno-economic analysis of microwave pyrolysis of sugarcane bagasse biochar production". *Biomass Conversion and Biorefinery*. **15** (9): 14229-14239. 10.1007/s13399-024-06232-7.
- [107] D. C. Makepa, C. H. Chihobo, W. R. Ruziwa, and D. Musademba. (2023). "Microwaveassisted pyrolysis of pine sawdust: Process modelling, performance optimization and economic evaluation for bioenergy



- recovery". *Heliyon*. **9** (3): e14688. <u>10.1016/</u> j.heliyon.2023.e14688.
- [108] I. Fonts, C. Lazaro, A. Cornejo, J. L. Sanchez, Z. Afailal, N. Gil-Lalaguna, and J. M. Arauzo. (2024). "Bio-oil Fractionation

According to Polarity and Molecular Size: Characterization and Application as Antioxidants". *Energy Fuels.* **38** (19): 18688-18704. 10.1021/acs.energyfuels.4c02641.